https://doi.org/10.5194/essd-2026-496
Preprint. Discussion started: 31 July 2026

Open Access Earth System Science Data Discussions

The Global Ocean Data Analysis Project version 3 (GLODAPv3) – an internally consistent biogeochemical data product for the world ocean

Nico Lange[1], Siv K. Lauvset[1], Brendan R. Carter[2,3], Matthew P. Humphreys[4], Ryan J. Woosley[5], Are Olsen[6], Henry C. Bittig[7], Alex Kozyr[8], Marta Álvarez[9], Kumiko Azetsu-Scott[10], Susan Becker[11], Peter J. Brown[12], Leticia Cotrim da Cunha[13], Larissa Dias[2,3], Mario Hoppema[14], Masao Ishii[15], Emil Jeansson[1], Akihiko Murata[16], Jens Daniel Müller[17,18,19], Fiz F. Pérez[20], Carsten Schirnick[21], Reiner Steinfeldt[22], Adam Ulfsbo[23], Anton Velo[20], and Toste Tanhua[21]

[1] NORCE Research AS, Bjerknes Centre for Climate Research, Bergen, Norway
[2] Cooperative Institute for Climate Ocean and Ecosystem Studies, University Washington, Seattle, Washington, USA
[3] Pacific Marine Environmental Laboratory, National Oceanic and Atmospheric Administration, Seattle, Washington, USA
[4] Department of Ocean Systems (OCS), NIOZ Royal Netherlands Institute for Sea Research, Texel, the Netherlands
[5] Center for Sustainability Science & Strategy, Department of Earth, Atmospheric & Planetary Sciences, Massachusetts Institute for Technology, Cambridge, Massachusetts, USA
[6] Geophysical Institute, University of Bergen and Bjerknes Centre for Climate Research, Bergen, Norway
[7] Leibniz Institute for Baltic Sea Research Warnemünde, Rostock, Germany
[8] NOAA National Centers for Environmental Information, Silver Spring, MD, USA
[9] Instituto Español de Oceanografía, IEO-CSIC, A Coruña, Spain
[10] Department of Fisheries and Oceans, Bedford Institute of Oceanography, Dartmouth, NS, Canada
[11] Scripps Institution of Oceanography, UC San Diego, San Diego, CA 92093, USA
[12] National Oceanography Centre, Southampton, UK
[13] PPG-Oceanografia, Faculdade de Oceanografia, Universidade do Estado do Rio de Janeiro, Rio de Janeiro (RJ), Brazil
[14] Alfred Wegener Institute Helmholtz Centre for Polar and Marine Research, Bremerhaven, Germany
[15] Meteorological Research Institute, Japan Meteorological Agency, Tsukuba, Japan
[16] Research Institute for Global Change, Japan Agency for Marine-Earth Science and Technology, Yokosuka, Japan
[17] Carbon to Sea Initiative, Washington, D.C., United States
[18] Climate and Environmental Physics, Physics Institute, University of Bern, Bern, Switzerland
[19] Oeschger Centre for Climate Change Research, University of Bern, Bern, Switzerland
[20] Instituto de Investigaciónes Mariñas, IIM – CSIC, Vigo, Spain
[21] GEOMAR Helmholtz Centre for Ocean Research Kiel, Kiel, Germany
[22] Institute for Environmental Physics, University of Bremen, Bremen, Germany
[23] Department of Marine Sciences, University of Gothenburg, Gothenburg, Sweden

Correspondence to: Nico Lange (nlan@norceresearch.no); Siv K. Lauvset (sivk@norceresearch.no)

https://doi.org/10.5194/essd-2026-496
Preprint. Discussion started: 31 July 2026

Open Access Earth System Science Data Discussions

Abstract

The Global Ocean Data Analysis Project (GLODAP) is a synthesis effort providing surface-to-bottom ocean biogeochemical observations determined through chemical analysis of discrete bottle samples, with an emphasis on seawater inorganic carbon chemistry and related variables. Version 3 of GLODAP comprises data from 1181 cruises, spanning more than 50 years of observations (1972 - 2023). It includes all data from the previous GLODAPv2.2023 (Lauvset et al., 2024) together with newly added data from 57 cruises. For all cruises, 13 core variables (temperature, salinity, oxygen, nitrate, silicate, phosphate, dissolved inorganic carbon, total alkalinity, CFC-11, CFC-12, CFC-113, CCl_4, and SF_6) have undergone extensive quality control with particular focus on the identification and removal of systematic differences between cruises. The data are available in two formats: (i) as submitted by the data originators, converted to World Ocean Circulation Experiment (WOCE) exchange format, and (ii) as a merged data product in which adjustments have been applied. These adjustments were determined using crossover analyses in combination with a newly developed global inversion method, the furthest-first routine. The applied adjustments are intended to remove systematic differences arising from differences in measurement methods, calibration, and/or data-handling practices, while preserving known or likely temporal trends and natural variability. The consistency of the adjusted data product is estimated to be 0.0013 for salinity, 0.7% for oxygen, 0.4% for nitrate, 0.5% for silicate, 0.5% for phosphate, 1.2 µmol kg^{-1} for dissolved inorganic carbon, and 1.4 µmol kg^{-1} for total alkalinity. Consistency estimates could not be derived for transient tracers, but they are believed to be consistent to better than 5% (10% for SF_6). The enhanced consistency enables different datasets to be used together with greater confidence. Newly introduced cruise-specific uncertainty estimates for all core variables provide more granular quantifications of remaining cruise-to-cruise inconsistencies. Additional variables, including pH, discrete CO_2 fugacity (fCO_2), isotopic tracers, and others, were not subjected to secondary quality control but are included in the data product.

The original data, their documentation (metadata), and DOIs are available through the Ocean Carbon and Acidification Data System (OCADS) of NOAA's National Centers for Environmental Information (NCEI), which also hosts the merged data product. All secondary quality control decisions and supporting information can be found in the online adjustment table (https://glodapv3.geomar.de, last accesses 26.06.2026). The product is distributed as a single global file and as four regional subsets (Arctic, Atlantic, Indian, and Pacific Oceans) under https://doi.org/10.25921/m6tp-mj50 (Lange et al., 2026). These adjusted files also include ancillary and approximated data obtained through interpolation or calculation from measured data.

https://doi.org/10.5194/essd-2026-496
Preprint. Discussion started: 31 July 2026

Open Access Earth System Science Data Discussions

1. Introduction

The global ocean plays a central role in Earth's climate system by absorbing most of the excess heat due to the increased greenhouse effect and about 30% of human carbon dioxide (CO_2) emissions, thereby moderating the pace of global warming (Friedlingstein et al., 2026). At the same time, this climate mitigation service comes at a cost: uptake of atmospheric CO_2 alters seawater carbonate chemistry and drives ocean acidification with consequences for marine ecosystems, biogeochemical cycling, and the long-term functioning of the ocean carbon sink (Doney et al., 2009; IPCC, 2021). Long-term observational data traceable to the highest metrological quality are required to document and understand these changes, and such data primarily comes from ship-based campaigns. Notable examples of such campaigns during the last decades include the Joint Global Ocean Flux Study (JGOFS; Fasham et al., 2001), the World Ocean Circulation Experiment (WOCE; Joyce, 1991), the Climate Variability and Predictability programme (CLIVAR; e.g., Smith et al., 2019), and the Global Ocean Ship-based Hydrographic Investigations Program (GO-SHIP; Talley et al., 2016; McDonagh et al., in press). While an expanding suite of autonomous platforms, such as Argo (Wong et al., 2020), has advanced our capacity to observe the ocean, such platforms have serious limitations which implies that full-depth ship-based observation campaigns are essential for calibrating and validating the data they produce

The objective of the Global Ocean Data Analysis Project (GLODAP) is to synthesize these ship-based, carbon relevant biogeochemical and hydrographic surface-to-bottom observations into a global, internally consistent, high-quality data product (Key et al., 2004; Olsen et al., 2016; Lauvset et al., 2024). By aggregating, quality controlling, and harmonizing data from many nations, expeditions, programs, and laboratories over the past 50 years, GLODAP increases accessibility, interoperability and scientific reproducibility for these data. A defining feature of the GLODAP synthesis is its focus on secondary quality-control where, when warranted, adjustments are applied to core variables (i.e., temperature, salinity, dissolved oxygen, macronutrients (phosphate, nitrate, silicate), dissolved inorganic carbon, total alkalinity, and halogenated transient tracers) in order to remove systematic measurement differences between cruises (Key et al., 2010; Olsen et al., 2016). Such differences between cruises may arise from a range of sources, such as preservation artifacts, changes in instrumentation, reference materials, or analytical calibration. By removing such systematic differences, GLODAP therefore helps ensure comparability among datasets and allows different data sets to be used together with greater confidence. As such, GLODAP is an open access, FAIR (Findable, Accessible, Interoperable, and Reusable; Wilkinson et al., 2016) data product that enables the study of global phenomena that cannot be robustly investigated from isolated datasets alone (Tanhua et al., 2021), such as quantification of the oceanic inventories of anthropogenic and natural carbon (e.g., Gruber et al., 2019; Keppler et al., 2023; Muller et al., 2023); ocean acidification (e.g., Carter et al., 2017; Müller et al., 2024); ventilation rates (e.g., Jeansson et al., 2021); oxygen levels (Stendardo and Gruber, 2012); and nutrient distributions (e.g., Carter et al., 2021). As independent evidence to the utility and value of the GLODAP effort, GLODAPv2 (Olsen et al., 2016) and its subsequent annual updates (e.g., Lauvset et al., 2024) have over 1000 citations combined (according to ESSD publication metrics) and GLODAPv1.1 (Key et al., 2004) has more than 1200 citations (according to AGU publication metrics).

Here we present GLODAPv3, the third full reevaluation of GLODAP cruises. International ship-based observation programs typically operate on decadal or longer timescales, but new data are made available for GLODAP annually. While GLODAPv2 was updated annually between2019 and 2023 by using the original product as a reference for additional cruises, an approximately decadal re-evaluation of all cruises and adjustments is warranted, in particular as data quality tends to increase with time (Lauvset et al., 2024). As planned, this release of GLODAPv3 coincides with the completion of the second GO-SHIP decade (2014-2023, McDonagh et al., in press). In addition, there is a strong user-driven demand for more robust quantification of the uncertainty of these data. Finally, there is a need to amend known issues in earlier versions. Here, we describe the data product, the underlying data assembly, and the revised secondary quality control (QC) framework. Further, we provide robust uncertainty and consistency estimates, granular information about the applied adjustments, and a brief comparison between GLODAPv2 and GLODAPv3.

https://doi.org/10.5194/essd-2026-496
Preprint. Discussion started: 31 July 2026

Open Access Earth System Science Data Discussions

2. Data and Methods

2.1. Data Sources

The GLODAPv3 synthesis is based on 1181 discrete cruise files, comprising all data included in GLODAPv2.2023 together with 57 newly submitted cruises. In addition to newly added cruises, several previously included datasets were updated and/or revised. Relevant information can also be found in the World Ocean Database (Garcia et al., 2026). We note that during data assembly, differences in file versions in different archives were identified for cruises already included in earlier GLODAP releases. In all cases the version at the Ocean Carbon and Acidification Data System (OCADS) at the National Oceanographic and Atmospheric Administration (NOAA) National Centers for Environmental Information (NCEI) was used as the source file for GLODAPv3. This ensures consistency in the assembly workflow for GLODAP, but the issue reflects the ongoing challenge of maintaining synchronized holdings across multiple public archives. While not in the scope of GLODAP we recommend that alignment between various data repositories be improved.

In line with the GLODAP objectives, all cruises must include either (i) data for at least one of the inorganic carbon variables, (ii) data for halogenated transient tracers, or (iii) data on a carbon isotope. The cruises in GLODAPv3 span all major ocean basins and five decades (1972-2023). Figure 1, Fig. 2, and Table 1 give an overview of the spatial and temporal distribution of the included cruises, including the number of cruises per basin and decade, and the number of samples available for each core variable. As in earlier versions, due to the nature of open ocean ship-based observations, a summer bias is present in the data (Lauvset et al., 2024, Fig. 10).

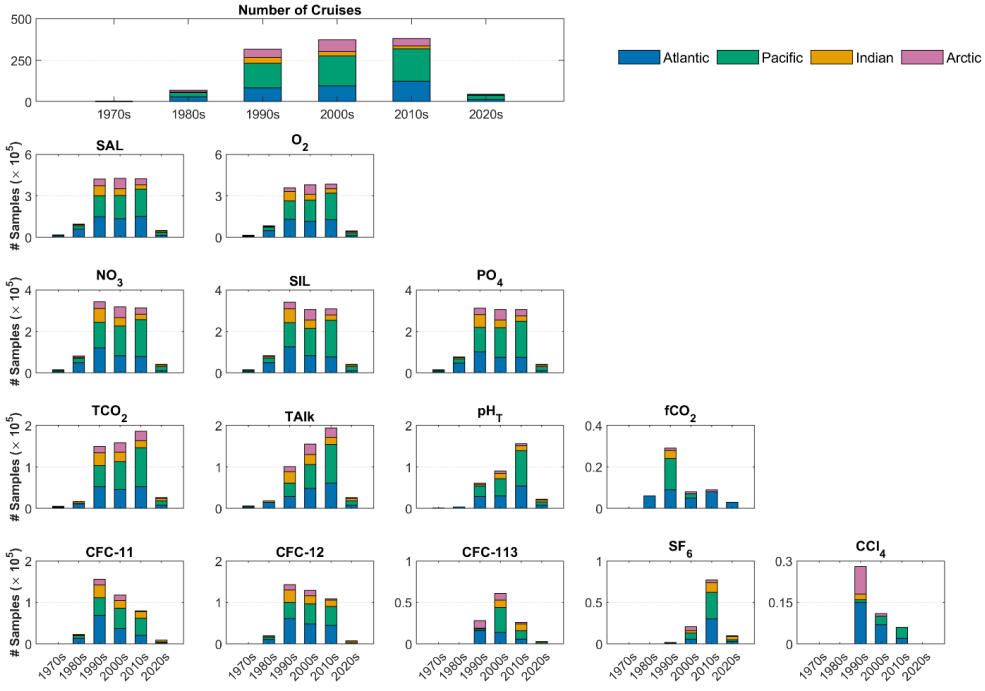

Figure 1: Decadal distribution of GLODAPv3 cruises and sample density per region. (Top row) Total number of cruises (1,181) conducted per decade. (Rows 2–5) Stacked decadal sample counts (x10^5) sorted by variable group. Colored bars differentiate regional contributions across the Atlantic, Pacific, Indian, and Arctic Oceans. Cumulative variable sample sizes (in millions) across the entire product are as follows: SAL (1.4), O_2 (1.2), NO_3 (1.1), SIL (1.1), PO_4 (1.1), TCO_2 (0.6), TAlk (0.5), pH (0.3), fCO_2 (0.05), CFC-11 (0.4), CFC-12 (0.4), CFC-113 (0.1), SF_6 (0.1), and CCL_4 (0.05).

https://doi.org/10.5194/essd-2026-496
Preprint. Discussion started: 31 July 2026

Open Access Earth System Science Data Discussions

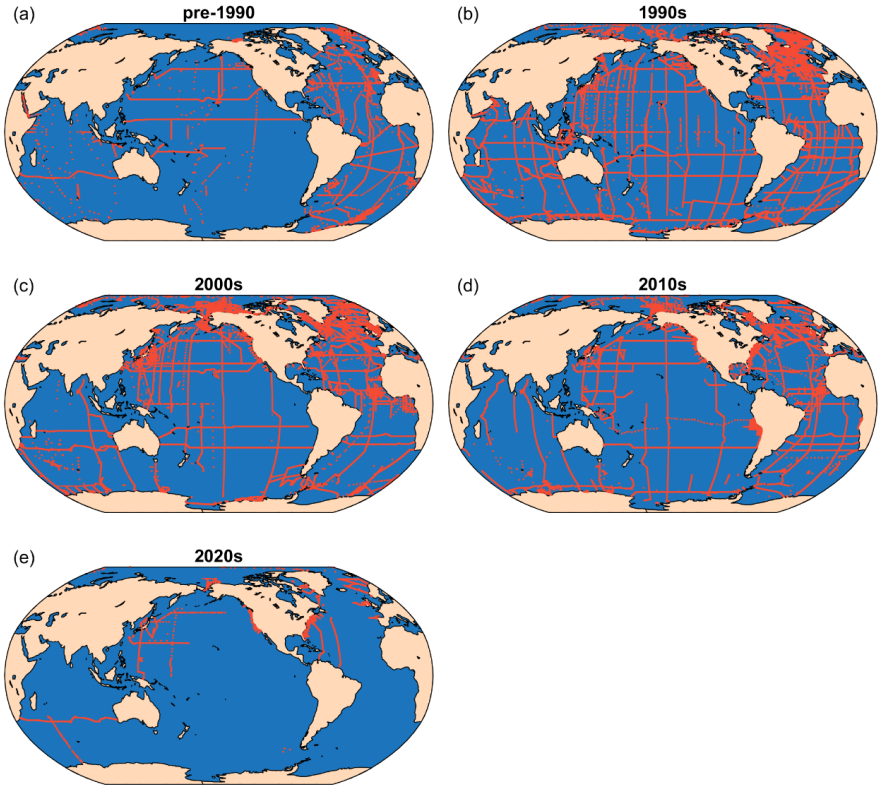

Figure 2: Spatial distribution of cruises in GLODAPv3, divided into the (a) pre-1990s, (b) 1990s, (c) 2000s, (d) 2010s, and (e) 2020s.

Table 1: Table listing the number of data points in GLODAPv3, as well as the number of data with various combinations of variables.

Variables	**Number of records**
All original core (salinity, oxygen, nitrate, silicate, phosphate, TCO_2, TAlk, pH, CFC-11, CFC-12, CFC-113, CCl_4, and SF_6)	174
All original core except SF_6	2037
Salinity, oxygen, nitrate, silicate, phosphate, CFC-11, CFC-12, CFC-113, CCl_4, and SF_6 plus two of TCO_2, TAlk, and pH	635
Salinity, oxygen, nitrate, silicate, phosphate, TCO_2, TAlk, pH	200 549
CFC-11, CFC-12, CFC-113, CCl_4, and SF_6	925
At least one halogenated transient tracer species or SF_6	442 785
SF_6	110 950
Two out of the three CO_2 chemistry original core variables (TCO_2, TAlk, pH)	495 738
Measured fCO_2	53 981
Salinity, oxygen, nitrate, silicate, and phosphate	938 660

https://doi.org/10.5194/essd-2026-496
Preprint. Discussion started: 31 July 2026

Salinity and oxygen	1 261 235
No salinity	55 333
Total in GLODAPv3	1 498 120

2.2 Methods

2.2.1 Format conversion and primary QC

Before archival at OCADS, all newly submitted data were converted to the WHP (WOCE Hydrographic Program) exchange bottle format and the associated WOCE flagging scheme was checked or introduced whenever needed. WHP-exchange is a comma-delimited ASCII (American Standard Code for Information Interchange) format for data from hydrographic cruises (Swift and Diggs, 2008). GLODAP only includes WHP-exchange in the bottle format with discrete data and CTD data at bottle trip depths. Within the WHP-exchange format the 'EXPOCODE', a combination of the ship's country and platform codes and the date of departure in the ISO8601 format (YYYYMMDD), is used as the unique identifier of each individual cruise. The country and platform codes were taken from the ICES (International Council for the Exploration of the Sea) library (https://vocab.ices.dk/, last access: 19 March 2026). The semantics (e.g., standardized variable names and units) are provided in Table 2 for the variables included in GLODAP. More detailed information about the WHP-exchange format can be found at https://exchange-format.readthedocs.io/ (v1.2.2 as of 2024, last access: 19 March 2026) and in the most recent GLODAPv2.2023 data description paper (Lauvset et al., 2024). Exchange file preparation required unit conversion in some cases for oxygen, from concentrations expressed as milliliters per liter (mL L^{-1}) to amount content expressed as micromoles per kilogram of seawater (µmol kg^{-1}). The factor 44.66 µmol O_2 mL^{-1} was used for the "milliliters of oxygen" to "micromoles of oxygen" conversion, while the density required for the "per liter" to "per kilogram" conversion was calculated from the reported salinity and draw temperatures whenever possible (following Jiang et al. (2022), otherwise potential density based on CTD data was used. Each data column, except pressure, which are assumed to be "good" if they exist, has an associated column of WOCE data flags (Joyce and Corry, 1994) as listed in Table 3. Missing numbers are indicated by −999, with an accompanied WOCE quality flag of 9. Lastly, for GLODAP's workflow, station and bottle numbers are required to be numeric, which led to conversions in some cases.

Because a meaningful secondary QC requires precise measurements, an additional primary QC was performed prior to the crossover analysis. This step was performed in addition to any primary QC performed by the data providers/generators. The primary QC itself relies upon inspection of property–property plots (Sabine et al., 2005; Tanhua et al., 2010) with outliers showing up in two or more different plots generally being considered suspicious. For this purpose, the AtlantOS QC software (Velo et al., 2021) was used, with inspection restricted to deep samples (>1000 m), where previously undetected outliers can challenge the secondary QC. Suspicious samples identified during this process were, where possible, communicated to the data originator for confirmation before being flagged in the original cruise file. Any data flagged 3 ("questionable") or 4 ("bad") were neglected during the secondary QC analyses and are excluded from the final product.

Table 2: Variables in the GLODAPv3 product files, their units, short and flag names, and corresponding names in the individual cruise exchange files.

Variable	Units	Product file name	WOCE flag name[a]	Secondary QC flag name[b]	WHP-exchange name
Expocode		expocode			EXPOCODE
Digital Object Identifier		doi			
Assigned sequential GLODAPv3 cruise number		cruise			

https://doi.org/10.5194/essd-2026-496
Preprint. Discussion started: 31 July 2026

Open Access Earth System Science Data Discussions

Variable	Units	Product file name	WOCE flag name[a]	Secondary QC flag name[b]	WHP-exchange name
GLODAPv2.2023 cruise number		cruisev2			
Basin identifier[c]		region			
Station		station			STNNBR
Cast		cast			CASTNO
Year		year			DATE
Month		month			DATE
Day		day			DATE
Hour		hour			TIME
Minute		minute			TIME
Latitude		latitude			LATITUDE
Longitude		longitude			LONGITUDE
Bottom depth	m	bottomdepth			
Pressure of the deepest sample	dbar	maxsampdepth			DEPTH
Niskin bottle number		bottle			BTLNBR
Sampling pressure	dbar	pressure			CTDPRS
Sampling depth	m	depth			
Temperature	°C	temperature	temperaturef	temperatureqc	CTDTMP
Potential temperature	°C	theta			THETA
Conservative temperature[d]	°C	constemperature			CTDCT
Practical Salinity[d]		salinity	salinityf	salinityqc	CTDSAL/SALNTY
Absolute salinity	g kg^{-1}	abssalinity	(salinityf)	(salinityqc)	DNSSAL
Potential density anomaly	kg m^{-3}	sigma0	(salinityf)		
Potential density anomaly, ref 1000 dbar	kg m^{-3}	sigma1	(salinityf)		
Potential density anomaly, ref 2000 dbar	kg m^{-3}	sigma2	(salinityf)		
Potential density anomaly, ref 3000 dbar	kg m^{-3}	sigma3	(salinityf)		
Potential density anomaly, ref 4000 dbar	kg m^{-3}	sigma4	(salinityf)		
Neutral density anomaly	kg m^{-3}	gamma	(salinityf)		
Oxygen	µmol kg^{-1}	oxygen	oxygenf	oxygenqc	CTDOXY/OXYGEN
Apparent oxygen utilization	µmol kg^{-1}	aou	aouf		
Nitrate	µmol kg^{-1}	nitrate	nitratef	nitrateqc	NITRAT
Nitrite	µmol kg^{-1}	nitrite	nitritef		NITRIT
Silicate	µmol kg^{-1}	silicate	silicatef	silicateqc	SILCAT
Phosphate	µmol kg^{-1}	phosphate	phosphatef	phosphateqc	PHSPHT

https://doi.org/10.5194/essd-2026-496
Preprint. Discussion started: 31 July 2026

Open Access Earth System Science Data Discussions

Variable	Units	Product file name	WOCE flag name[a]	Secondary QC flag name[b]	WHP-exchange name
Total dissolved inorganic carbon (TCO_2) (measured)[c]	µmol kg^{-1}	tco2	tco2f	tco2qc	TCARBN
Total dissolved inorganic carbon (calculated)	µmol kg^{-1}	tco2calc			
Total titration seawater alkalinity (TAlk)[c]	µmol kg^{-1}	talk	talkf	talkqc	ALKALI
Total titration seawater alkalinity (calculated)	µmol kg^{-1}	talkcalc			
pH on total scale, 25° C and 0 dbar of pressure		phts25p0	phts25p0f		PH_TOT
pH on total scale, in situ temperature and pressure		phtsinsitutp	phtsinsitutpf		PH_INSITU
pH original scale		phorscale			
pH original temperature	°C	phortemperature			PH_TMP
pH on total scale, 25° C and 0 dbar of pressure (calculated)		phts25p0_calc			
fCO_2 at 20° C and 0 dbar of pressure	µatm	fco2	fco2f		FCO2/PCO2
fCO_2 original temperature [f]	°C	*f*co2temp	(fco2f)		FCO2_TMP/PCO2_TMP
fCO_2 at 20° C and 0 dbar of pressure (calculated)	µatm	fco2calc			
CFC-11	pmol kg^{-1}	cfc11	cfc11f	cfc11qc	CFC-11
Partial pressure of CFC-11	ppt	pcfc11	(cfc11f)		
CFC-12	pmol kg^{-1}	cfc12	cfc12f	cfc12qc	CFC-12
Partial pressure of CFC-12	ppt	pcfc12	(cfc12f)		
CFC-113	pmol kg^{-1}	cfc113	cfc113f	cfc113qc	CFC-113
Partial pressure of CFC-113	ppt	pcfc113	(cfc113f)		
CCl_4	pmol kg^{-1}	ccl4	ccl4f	ccl4qc	CCL4
Partial pressure of CCl_4	ppt	pccl4	(ccl4f)		
SF_6	fmol kg^{-1}	sf6	sf6f	sf6qc	SF6
Partial pressure of SF_6	ppt	psf6	(sf6f)		
$\delta^{13}C$	‰	c13	c13f	c13qc	DELC13
$\Delta^{14}C$	‰	c14	c14f		DELC14
$\Delta^{14}C$ counting error	‰	c14err			C14ERR
^{3}H	TU	h3	h3f		TRITIUM
^{3}H counting error	TU	h3err			TRITER

https://doi.org/10.5194/essd-2026-496
Preprint. Discussion started: 31 July 2026

Variable	Units	Product file name	WOCE flag name[a]	Secondary QC flag name[b]	WHP-exchange name
δ^3He	%	he3	he3f		DELHE3
^{3}He counting error	%	he3err			DELHER
He	nmol kg^{-1}	he	hef		HELIUM
He counting error	nmol kg^{-1}	heerr			HELIER
Ne	nmol kg^{-1}	neon	neonf		NEON
Ne counting error	nmol kg^{-1}	neonerr			NEONER
δ^{18}O	‰	o18	o18f		DELO18
Total organic carbon	µmol L^{-1} [g]	toc	tocf		TOC
Dissolved organic carbon	µmol L^{-1} [g]	doc	docf		DOC
Dissolved organic nitrogen	µmol L^{-1} [g]	don	donf		DON
Dissolved total nitrogen	µmol L^{-1} [g]	tdn	tdnf		TDN
Chlorophyll *a*	µg kg^{-1} [g]	chla	chlaf		CHLORA

[a]The only derived variable assigned a separate WOCE flag is AOU as it depends strongly on both temperature and oxygen (and less strongly on salinity). For the other derived variables, the applicable WOCE flag is given in parentheses. [b]Secondary QC flags indicate whether data have been subjected to full secondary QC (1) or not (0), as described in Sect. 2.2.1. [c]1 is the Atlantic Ocean, 4 is the Arctic Mediterranean Sea (i.e., the Arctic Ocean plus the Nordic Seas), 8 is the Pacific Ocean, and 16 is the Indian Ocean. [d]Calculated using TEOS-10. [e]For consistency with GLODAP legacy we are using TCO_2 and TAlk for total dissolved inorganic carbon and total titration seawater alkalinity, respectively. [f]Included for clarity, is 20 °C for all occurrences. [g]Units have not been checked; some values in micromoles per kilogram (for TOC, DOC, DON, TDN) or microgram per liter (for Chl *a*) are probable.

Table 3: WOCE flags in GLODAPv3 exchange-format original data files (briefly; for full details see Swift, 2010) and the simplified scheme used in the merged product files.

WOCE flag value	Interpretation	
	Original data exchange files	Merged product files
0	Flag not used	Interpolated value
1	Data not received	Flag not used[a]
2	Acceptable	Good data
3	Questionable	Flag not used[b]
4	Bad	Flag not used[b]
5	Value not reported	Flag not used[b]
6	Average of replicate	Flag set to 2[c]
7	Manual chromatographic peak measurement	Flag set to 2[c]
8	Irregular digital peak measurement	Flag not used[b]
9	Sample not drawn	No data

[a]Flag set to 9 in product files [b]Data are not included in the GLODAPv3 product files and their flags reassigned to 9. [c]Data are included, but flag set to 2

2.2.2 Merging of sensor and bottle data for salinity and oxygen

Salinity and oxygen data can be obtained by analysis of water samples (discrete bottle data) and by using sensor technology. Salinity is measured using the conductivity cell of the CTD sensor, and oxygen is measured using either electrochemical or optical sensors. For GLODAPv3, bottle and sensor data were merged prior to the secondary QC, ensuring that as many data points as possible include these variables. Ideally, both data types are present in all data files, and the sensor data have been calibrated using the water samples, such that the sensor data can easily be merged in to fill gaps in the bottle data. However, experience from GLODAPv2 shows that this is not always the case (Olsen et al., 2016).

The merging procedures in GLODAPv3 were identical with the methodology applied in GLODAPv2, which accounted for seven possible scenarios (Action-IDs, Table 4). All datasets were reevaluated by visually inspecting the linear fit between the discrete bottle and CTD data, and the coefficient of determination (r^2) and root-mean

https://doi.org/10.5194/essd-2026-496
Preprint. Discussion started: 31 July 2026

squared error for data deeper than 1000 m. Compared to GLODAPv2.2023, 66 cruises have a different salinity Action-ID and 64 cruises have a different oxygen Action-ID in GLODAPv3. In all cases, this is because the Action-ID in GLODAPv2 appeared incorrect (e.g., an Action-ID '3' was given to cruises where no bottle data are available). As in previous versions, the extent to which the bottle data are mislabeled sensor data is uncertain.

Table 4: Summary of salinity and oxygen calibration needs and actions. The number of cruises within each of the scenarios is identified.

Action-ID	Description	Salinity	Oxygen
1	No data are available: no action needed.	1	93
2	No bottle values are available: use CTD values.	198	77
3	No CTD values are available: use bottle values.	254	660
4	Too few data of both types are available for comparison and >80% of the records have bottle values: use bottle values.	0	0
5	The CTD values do not deviate significantly from bottle values: replace missing bottle values with CTD values.	623	284
6	The CTD values deviate significantly from bottle values: calibrate CTD values using linear fit and replace missing bottle values with calibrated CTD values.	141	74
7	The CTD values deviate significantly from bottle values, and no good linear fit can be obtained for the cruise: use bottle values and discard CTD values.	8	37

2.2.3 pH and *f*CO2

Although great efforts were made and many discussions were held on possible alternative methods for applying secondary QC to pH, it was decided that the best course of action at the present time was to not apply secondary QC (Sect. 4.1). Instead, pH measurements are provided with only primary QC and all values being converted to the total pH scale, pH_T, at both standard (25 °C and surface (0 dbar) pressure) and in situ (temperature and pressure) conditions. The scale conversion followed the methods described in Olsen et al. (2019) with the exception that CO2SYSv3 (Sharp et al., 2020) was used instead of CO2SYSv2 (Humphreys et al., 2022). The carbonate system was parameterized using the carbonic acid dissociation constants of Lueker et al. (2000), the total boron to salinity ratio of Lee et al. (2010), the hydrogen fluoride dissociation constant of Perez and Frage (1987), and the hydrogen sulfate dissociation constant of Dickson (1990). For traceability and reproducibility of the carbonate system calculations, ancillary columns indicate the measurement scale and temperature reported in the original datasets.

Based on assessments of random and systematic uncertainties using GLODAPv2.2022 spectrophotometric pH data, the total uncertainty in pH_T is thought to be ~0.011, although some sub-sets have lower (e.g., spectrophotometric measurements using purified indicator dye) or higher (e.g., potentiometric measurements) uncertainties (Carter et al., 2024a). This uncertainty value is slightly higher than the minimum adjustment value of 0.010 used for GLODAPv2 starting in v2.2019 and subsequent updates (Olsen et al., 2019) and twice that used (0.005) in the original GLODAPv2 (Olsen et al., 2016). The cruises flagged as poor quality (-777) and excluded from the dataset in prior versions were re-evaluated in light of our increased uncertainty understanding. As a result, nine previously excluded cruises are now retained in the product.

Separate to observed pH_T, the data product includes pH_T values calculated from dissolved inorganic carbon (TCO_2) and total alkalinity (TAlk) at standard conditions. These calculations were performed using CO2SYSv3 with the same constants as described above. The random uncertainties in these calculated values (using v2.2022) have been assessed to be ~0.008 (Carter et al., 2024a). Systematic uncertainties such as from the choice of constants used in the calculations have not been evaluated and should be considered when using these values.

Following analogous reasoning, no secondary QC was applied to discrete fugacity of CO_2 (fCO_2) data, fCO_2 measurements are provided with only primary QC. All values were converted to 20 °C and 0 dbar pressure using CO2SYSv3. Similarly, CO2SYSv3 was also used for the conversion of partial pressure of CO_2 (pCO_2) to fCO_2 for the 52 cruises where pCO_2 was reported. The procedures for these conversions were the same as for the pH conversions. For 10 cruises no temperature information could be obtained, and the corresponding fCO_2 values

https://doi.org/10.5194/essd-2026-496
Preprint. Discussion started: 31 July 2026

were not included in the product. As for pH_T, the data product includes separate fCO_2 values calculated from TCO_2 and TAlk at standard conditions (20 °C and 0 dbar). For traceability and reproducibility of the carbonate system calculations, ancillary columns indicate the temperature reported in the original datasets. Based on assessments of random and systematic uncertainties using GLODAPv2.2022 fCO_2 data, the total uncertainty in fCO_2 is thought to be ~2% (Carter et al., 2024a).

2.2.4 Secondary QC Procedure: Crossover Analysis and Inversion

The secondary QC of temperature, salinity, oxygen, macronutrients, TCO_2, andTAlk was carried out as a multi-step procedure inspired by the routines used for GLODAPv2 (Olsen et al., 2016). First, a crossover analysis in the deep ocean (Sect. 2.2.4.1) was used to determine differences (cruise-pair offsets') between cruises by comparing data where two different cruises overlap within a radius of 300 km, and both have data deeper than 1500 dbar. Second, the cruise-pair offsets were evaluated by the group of experts who determined pre-inversion adjustments which were subsequently applied to update the cruise-pair offsets. Pre-inversion adjustments are used either for very large individual cruise-pair offsets or for collections of cruises which are offset compared to (almost) everything else. In both cases a pre-inversion adjustment is only applied when there is consensus in the group of experts as to the cause of the bias (e.g., when different measurement or calibration procedures were used and resulted in consistently different offsets). Third, the inversion step (Sect. 2.2.4.2) organizes all cruise-pair offsets into a system of linear equations which is solved for the set of adjustments that, when applied to each cruise and variable, minimizes their average offset. Here, a statistical analysis informed by oceanographic knowledge (e.g., about properties or regions where deep ocean variability is expected) was included to decide on a subset of the inversion-derived adjustments to apply. Note that the final adjustments are only applied to the data in the product, not to the original cruise files. The possible outcomes of this multi-step procedure are detailed in Table 5.

Figure 3 describes the implementation of the above three steps to GLODAPv3. After primary QC all cruises are subjected to a crossover analysis. The resulting cruise-pair offsets are then organized into three different systems of equations ('matrices'): one for the northern North Atlantic ('NNATL'), one for the Arctic Mediterranean Seas ('Arctic', i.e., the Nordic Seas, Nansen Basin, Amundsen Basin, Canada Basin, Makarov Basin, Baffin Bay, and Davis Strait), and one for the remaining ocean ('Global'). The 'Arctic' is separated out as the sparsity of cruises and crossovers between these cruises makes it impossible to find a solution to the matrix of equations. Thus, instead of inversion step, final adjustments were determined based on the existing cruise-pair offsets, multilinear regressions, and deep water averages following Becker et al. (2016). Each sub-basin was evaluated separately.

The reasons for separating out the 'NNATL' are more complex than for the Arctic: The cruises in GLODAP are not evenly distributed in space, but rather clustered. There is a relatively large cluster of data in the 'NNATL', particularly in the Labrador Sea, which is poorly connected to the rest of the Atlantic Ocean. In addition, the 'NNATL' is a region exhibiting strong natural variability and deep winter ocean convection which means that there are quite strong anthropogenic trends in our core variables in the entire water column. As a result, the cruise-pair offsets here are often large, but also often uncertain. To avoid this region unnecessarily biasing the result of the inversion step, a sequential inversion approach is applied. First, the 'Global' matrix is solved to obtain a set of adjustments. These adjustments are then applied to cruises in the 'NNATL' subset that are also present in the 'Global' domain. In the subsequent solution of the 'NNATL' equation matrix, these previously adjusted cruises are included as fixed observations; that is, they contribute to the NNATL inversion but are not permitted to receive additional adjustments. This procedure ensures that the NNATL solution is constrained by the 'Global' adjustments, enforcing consistency between the two domains.

https://doi.org/10.5194/essd-2026-496
Preprint. Discussion started: 31 July 2026

Open Access Earth System Science Data Discussions

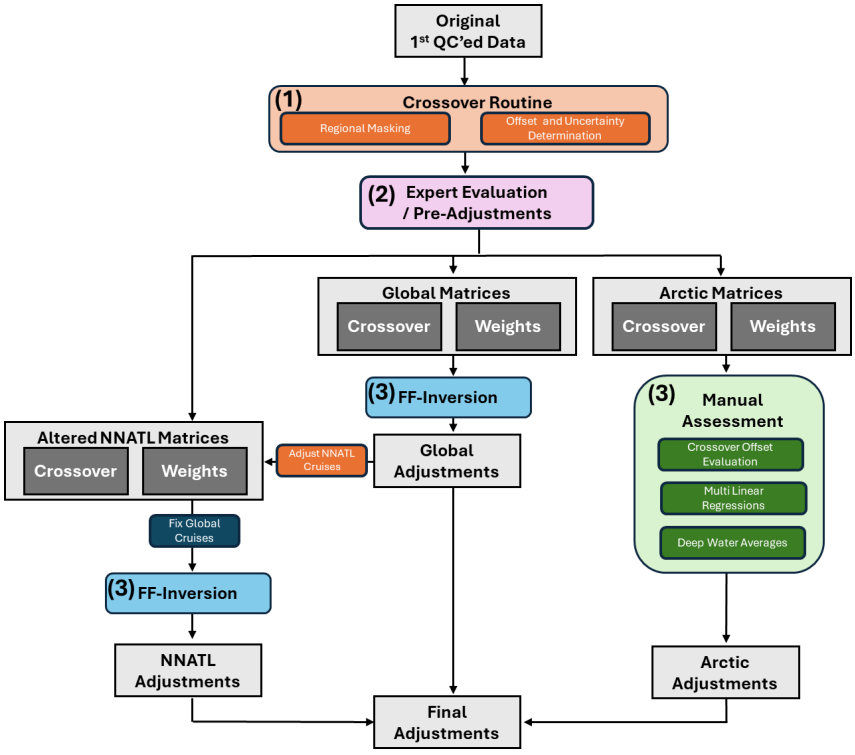

Figure 3: Flowchart displaying the general secondary QC procedure. Numbers in brackets correspond to the mentioned steps in the secondary QC procedure.

Table 5: Possible outcomes of the secondary QC and their codes in the online adjustment table and in the product.

Secondary QC result	Code	Product QC flag
The data are of good quality, are consistent with the rest of the dataset and should not be adjusted.	0/1[a]	1
The data are of good quality but are offset: adjust by adding (for salinity, TCO_2, TAlk, pH_T) or by multiplying (for oxygen, nutrients, CFCs) the adjustment value	Adjustment value	1
The data are of poor quality and excluded from the data product.	-777	NA
The data appear of good quality, but their nature, being from shallow depths and coastal regions without crossovers or similar, prohibits full secondary QC	-888	0
No data exist for this variable for the cruise in question	-999	NA

[a]The value of 0 is used for variables with additive adjustments (salinity, TCO_2, TAlk, pH_T) and 1 for variables with multiplicative adjustments (for oxygen, nutrients, CFCs). This is mathematically equivalent to 'no adjustment' in both cases.

2.2.4.1 Crossover Analysis

As for GLODAPv2 the crossover analyses were conducted using the "running-cluster" routine described by Tanhua et al. (2010) and implemented in the MATLAB gv2_x package (https://github.com/GLODAP/glodap.github.io/tree/main/docs/gv2_x, last accessed 26.06.2026). This procedure performs a station-by-station comparison between two cruises (A and B, Fig. 4). For each station of cruise A its vertically interpolated profile (using a quasi-Hermetian piecewise polynomial) is compared to each interpolated profile from all cruise B stations that are within 300 km distance. Using only data below 1500 dbar (or 2000 dbar

https://doi.org/10.5194/essd-2026-496
Preprint. Discussion started: 31 July 2026

for the 'NNATL' and the Arctic), difference-profiles for temperature, salinity, TCO_2, and TAlk and ratio-profiles for oxygen and macronutrients are then calculated for each station pair (grey lines in Fig. 4d, g, and j). The choice of depth cutoff reflects a trade-off between maximizing the number of available crossovers and minimizing the influence of natural variability and anthropogenic trends on the offsets.

Using all difference-profiles (or ratio-profiles), the routine calculates a mean (with standard deviation) difference profile (red dots and lines in Fig. 4d, g , and j), which is then used to calculate a weighted mean cruise-pair offset and standard deviation (green lines in Fig. 4d, g, and j; corresponding values shown in Fig. 4k). The weighting accounts for the scatter in the data, such that stations with low scatter contribute more to the mean than stations with high scatter, irrespective of whether the scatter arises from natural variability or measurement precision. To ensure robust results, the crossover analysis is performed in three different depth spaces: pressure, potential temperature (θ), and sigma-4 (σ_4). A weighted mean offset is calculated for each depth space, and the one based on most data and profiles was used as the 'cruise-pair offset' for the A-B cruise-pair. If all depth spaces have approximately the same amount of data and profiles, the average is used as 'cruise-pair offset'. Note that for temperature and salinity only the pressure space is used. The crossover analysis is conducted for all cruises, and the outcome is a vector containing all A-B 'cruise-pair offsets' and all B-A 'cruise-pair offsets', the latter being the negative of the former. Figure 4 shows, as an example, the result of a crossover between the cruises 06MT19970707 (A) and 18HU19960512 (B).

https://doi.org/10.5194/essd-2026-496
Preprint. Discussion started: 31 July 2026

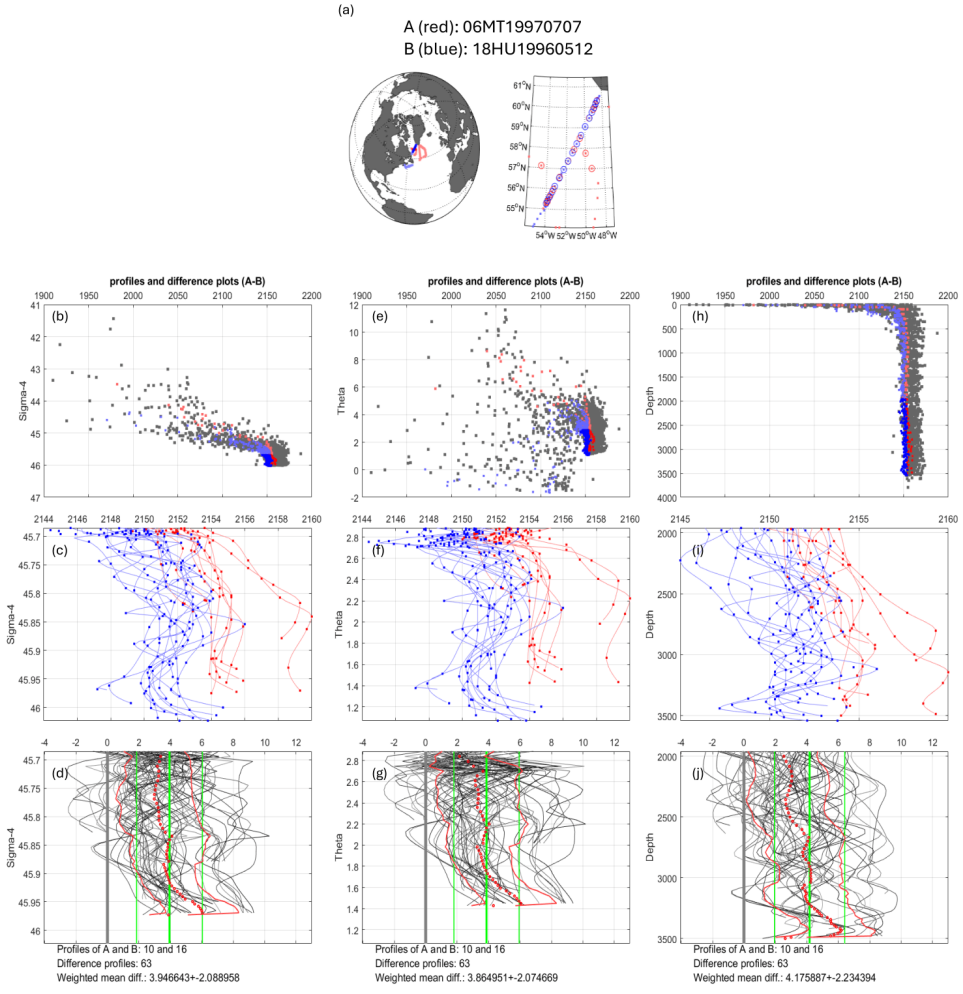

(k)	Offset (umol/kg)	O.Stdev (umol/kg)	Ratio	R.Stdev	Rating
Sigma-4	3.947	2.089	1.002	0.001	4
Theta	3.865	2.075	1.002	0.001	4
Pressure	4.176	2.234	1.002	0.001	4
Favorite	3.996	2.133	1.002	0.001	4

Figure 4: Summary figure for the crossover between cruises 06MT19970707 (A) and 18HU19960512 (B), for TCO_2 data. (a) shows maps of the cruises and the crossover stations. Panels (b-d) show TCO_2 data and profiles in sigma 4 space, (e-g) in theta space, and (h-j) in pressure space. For each of these spaces, the top row shows all nearby data for the full depth column (grey), cruise A (red), and cruise B (blue); the second row shows the crossover station profiles used for the analysis; and the bottom row shows the crossover result with grey lines indicating station difference profiles, red dots showing the mean offset at each depth (+/- standard deviation), and green vertical lines indicating the cruise-pair weighted mean offset (+/- standard deviation). (k) provides a summary table for the cruise-pair. All depth spaces show consistent results, and all have adequate data. The cruise-pair offset (average of all three depth spaces) is approximately 4 µmol kg^{-1}, with cruise A (red) showing higher TCO_2 concentrations than cruise B (blue). This is a significant difference.

https://doi.org/10.5194/essd-2026-496
Preprint. Discussion started: 31 July 2026

Based on the analyses in GLODAPv2 it is known that for some cruises one part of the cruise is offset relative to another. The regular crossover analysis is not able to capture this, so we introduced a 'spatial breakpoint analysis' to identify such intra-cruise offsets. This breakpoint analysis used all cruise-pair offsets for a given cruise and identified whether these show statistically significant (using the silhouette score; Rousseeuw, 1987) spatial clustering in latitude or longitude space. A maximum of one breakpoint per cruise was allowed, and for 17 cruises at least one variable indicated two distinct clusters. These cruises were then manually inspected, and 7 cruises were subsequently split up and the crossover analysis was then re-run. This practice allows for detection and adjustment of mid-cruise measurement shifts that might be expected from, for example, changes in calibration materials, equipment, or operators.

2.2.4.2 Inversion

The outcome of the crossover analysis can be presented as a system of linear equations in the form **Ax-b=r**, where **b** is a vector with the *o* cruise-pair offsets, **x** is a vector of the *n* adjustments for all *n* cruises, **A** is the *o* by *n* model matrix, and **r** is a vector with the *o* cruise-pair residuals. To account for the fact that not all offsets are equally robust we also use a weight, **W**, for each cruise-pair offset. The weights equal the squared inverse of the cruise-pair offset standard deviations, meaning that crossovers with high standard deviation receive low weight. The squared inverse standard deviation is further scaled by (i) the time difference between the two cruises involved in the crossover (with smaller differences providing higher weights), (ii) a crossover rating (1-5, with 5 being best) reflecting the number of profiles and deep samples used to calculate the cruise-pair offset, and (iii) the spatial density gradient, estimated from temperature and salinity climatologies (Reagan et al., 2023), in the area of the crossover. (i)-(iii) are first normalized to a range from 1 to 3 with low numbers reflecting high confidence in the crossover and then multiplied together and rescaled to a single number between 1 and 2, which is then multiplied to the squared inverse standard deviation. Figure 5 shows the impact applying the scaling factors has on the solution (**x**). On average, across all cruises the impact is minimal, but for some cruises scaling the weight reduces the suggested adjustment by more than 1 µmol kg^{-1} and in very rare cases by more than 2 µmol kg^{-1}.

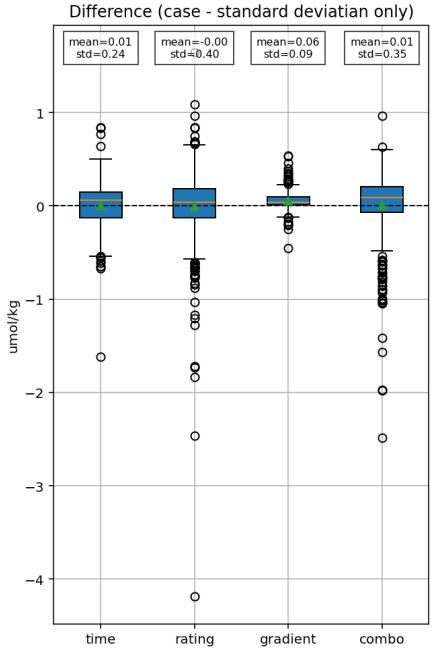

Figure 5: The impact of the three scaling factors, as well as their product, have on the adjustments for TCO_2 suggested by the FF inversion routine. The impact is presented as the difference between using only the inverse standard deviation as weight and scaling that by the additional factors.

https://doi.org/10.5194/essd-2026-496
Preprint. Discussion started: 31 July 2026

In earlier versions of GLODAP the system of equations was solved using a weighted least squares (WLSQ) matrix inversion following Johnson et al., (2001). However, in GLODAPv3 the system of equations is more overdetermined ($o >> n$) than it was in earlier versions, and because the cruise-pairs tend to be more clustered (most cruises have few cruise-pairs while a few have many) there is a high degree of multicollinearity (i.e., the cruise-pair offsets in **b** are not independent of each other). This, along with known weaknesses such as sensitivity to outliers and data groupings, means that the WLSQ method is ill-suited to find an optimal solution. These issues were, to a lesser degree, present also in GLODAPv2 and were then solved by doing regional inversions for the three major ocean basins (Atlantic, Indian, and Pacific) or inversions for regional groups of cruises, rather than finding one global solution. For GLODAPv3 we instead apply an iterative coordinate descent optimization method as implemented in the Furthest-First (FF) algorithm (Humphreys et al., 2026).

There are several steps to the FF routine as illustrated in Fig. 6.

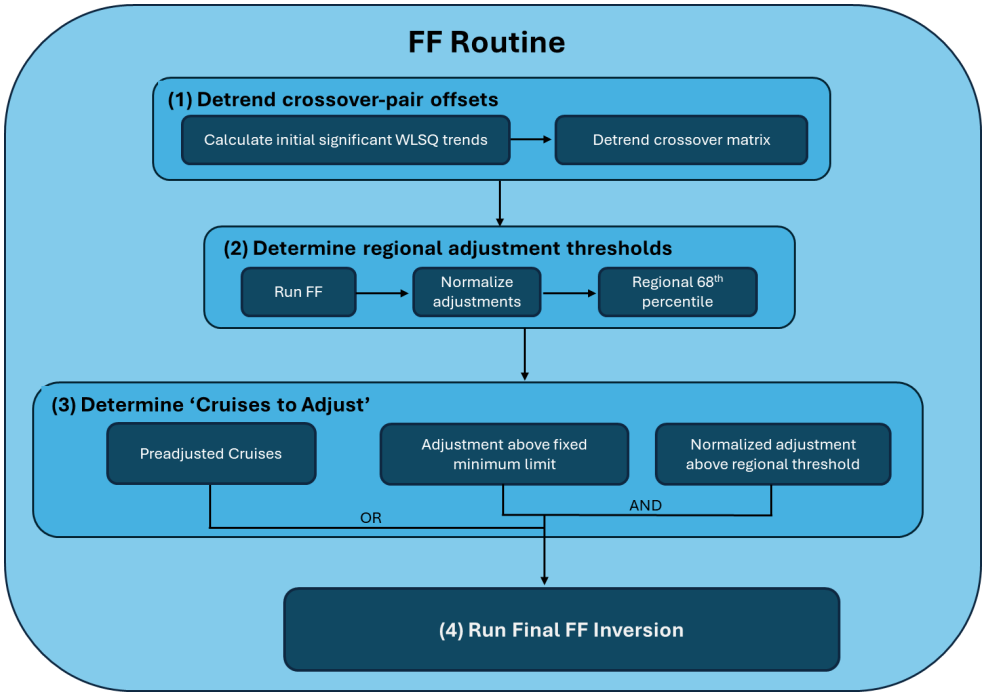

Figure 6: Flow chart displaying the three main processes within the FF routine.

In step 1, the cruise-pair offsets in **b** are detrended. This is necessary in order to preserve anthropogenic trends because otherwise the routine will act to remove them, and even though anthropogenic trends are small in the deep ocean we cannot assume they are negligible. To detrend **b**, we first identified the trends using a WLSQ linear regression applied to all cruise-pair offsets for a given cruise. If the trend, α, exceeded its standard error times 1.96 (the 2σ level) it was kept, and otherwise it was set to zero. The detrended cruise-pair offsets, **b'**, were then calculated for each cruise by subtracting $\alpha\Delta T$ from **b**, where ΔT is the time difference between all cruise-pair offsets for that cruise (Fig. 7).

In step 2, adjustments are determined using an iterative process. At each iteration step the cruise weighted mean offset (CWMO, Eq. 1) was calculated and, to avoid adjusting highly uncertain offsets, divided by its standard error. The CWMO is the weighted mean of all **r** for a given cruise, assuming that at step zero (i.e., before iterations

https://doi.org/10.5194/essd-2026-496
Preprint. Discussion started: 31 July 2026

begin) **r**=**b'** for all cruises. At each iteration the cruise with the largest normalized CWMO is adjusted, and all CWMOs subsequently recalculated. Since all CWMOs are recalculated at each step of the iteration there will be a residual CWMO for cruises that have been adjusted, which is then adjusted in a later step when it is once again the largest. The final adjustment is thus the cumulative adjustment for each cruise after the final iteration. For details on this iterative process see Humphreys et al. (in prep). Note that we use a cruise-pair offset only when (i) the crossover rating is above 3 (on a scale from 1-5); (ii) the range of the three depth space offsets is smaller than the lower absolute adjustment limit; and (iii) neither cruise in the pair is flagged -777. If any of these criteria fail, then that cruise-pair offset is removed from the CWMO calculation to limit the influence of highly uncertain cruise-pair offsets.

$$\bar{x} = \sum \frac{Wr}{W} \qquad (1)$$

Where $\bar{x}$ is the CWMO of cruise i, ***r*** are the cruise-pair residuals for cruise i and W are the corresponding weights, and the calculation is performed for each cruise at each iteration step.

In step 2, the iterations are run with all cruises allowed to adjust until the CWMO reaches 5% of the fixed minimum adjustment limit (Table 6). The result is used to determine regional adjustment thresholds (Table 7) that account for varying magnitudes of natural variability in different regions. Specifically, these thresholds are derived from the final adjustments normalized by their corresponding standard errors, with the threshold in each region defined as the 68th percentile (1σ) of the normalized adjustment magnitude.

In step 3, we identify a 'Cruises-to-Adjust' list. This list includes cruises identified for pre-inversion adjustments as well as cruises that satisfy all of the following criteria:
(i) the final normalized adjustment in step 2 exceeds the regional threshold (Table 7)
(ii) the final adjustment in step 2 exceeds the fixed minimum adjustment limits (Table 6);
(iii) the cruise has at least three cruise-pairs; and
(iv) neither the weighted nor the unweighted standard deviation of the CWMO is below the global 5th-percentile of the CWMO standard deviations.
Cruises failing criteria (iii) and/or (iv) were assigned a −888 flag (Table 5) and the secondary qc flag in the product files set to 0. For TCO_2 and TAlk, criteria (i)-(iv) were also applied to cruise-pair offsets identified for salinity-normalized data. If the adjustment suggested for salinity-normalized TCO_2 and/or TAlk did not satisfy all criteria, the cruise was excluded from the 'Cruises-to-Adjust' list, even if the adjustment for actual TCO_2 and TAlk did.

In step 4, another iterative process was run where only cruises on the 'Cruises-to-Adjust' list were eligible for adjustment, and no additional adjustment restrictions were imposed. This final step is necessary to ensure that the applied set of adjustments is optimal, accounting for the fact that not all cruises will be adjusted.

The iterative process of the FF method works in such a way as to maximize consistency within clusters of cruises first, and then, with very small adjustments at each iteration, moves the clusters towards global convergence. In the GLODAP network of cruises this happens by shifting all other clusters towards the cluster of cruises in the northwest Pacific Ocean, which is by far the largest (both in terms of cruises and crossovers). This FF solution correlates very well with the global WLSQ solution (Humphreys et al., 2026). We are unable to identify a physical or biogeochemical reason to expect systematic biases solely based on the cruises being in different ocean basins. We therefore, in step 2, choose to stop the iterative process once a solution is found that creates convergence within relatively large-scale clusters representing ocean sub-basins (Sect. 4.2). The final FF solution consists of an adjustment for each cruise, as well as an uncertainty for this adjustment.

Table 6: Fixed minimum adjustment limits and analytical precision. The adjustment limits represent the minimum offset that can be confidently established relative to the crossover analysis uncertainty (precision, natural variably, and inherent method uncertainties) for the variables considered. Note that the values provided for the analytical precision represent target values, i.e., not all cruises achieve this level of precision.

Variable	Minimum adjustment	Target Precision[a]
Salinity	0.0025	0.0004 (0.002)[b]

https://doi.org/10.5194/essd-2026-496
Preprint. Discussion started: 31 July 2026

Oxygen	0.5 %	0.1 % (2 %)[b]
Nutrients	1 %	0.4 % (0.6 %)[c]
TCO_2	2 µmol kg^{-1}	1 µmol kg^{-1}
TAlk	2 µmol kg^{-1}	1 µmol kg^{-1}
CFCs	5 % (10 %)[d]	2 % (3 %)[d]

[a]The GO-SHIP repeated hydrography manuals are the main source for the numbers provided. Other sources are the IOCCP-JAMSTEC 2018 Nutrients Intercomparison Report and Heuze et al., 2023. [b]The number in brackets refers to the analytical precision of CTD measurements. [c]The number in brackets refers to the analytical precision of phosphate measurements. [d]The number in brackets refers to SF_6.

Table 7: Regional normalized thresholds used to determine the 'Cruises-to-Adjust' list. Values shown correspond to the absolute adjustment divided by the total uncertainty. Only cruises with normalized adjustments above this value and an absolute adjustment above the fixed minimum are allowed to be adjusted in the third step of the FF routine. The higher the value the more robust the adjustment.

	SAL	**O_2**	**NO_3**	**SIL**	**PO_4**	**TCO_2**	**TAlk**
North Pacific	2.0	2.2	3.4	2.8	3.9	2.8	2.8
South Pacific	1.5	2.1	2.3	2.7	3.4	2.1	2.5
NNATL	1.2	2.1	1.4	2.0	1.9	2.0	1.2
North Atlantic	1.8	3.0	2.1	2.0	2.3	2.0	2.3
South Atlantic	1.7	2.4	2.2	1.7	2.1	1.8	1.8
Indian Ocean	1.5	1.4	1.6	1.9	2.0	1.8	2.6
Southern Ocean	1.4	1.9	2.4	1.7	2.0	1.9	2.3

https://doi.org/10.5194/essd-2026-496
Preprint. Discussion started: 31 July 2026

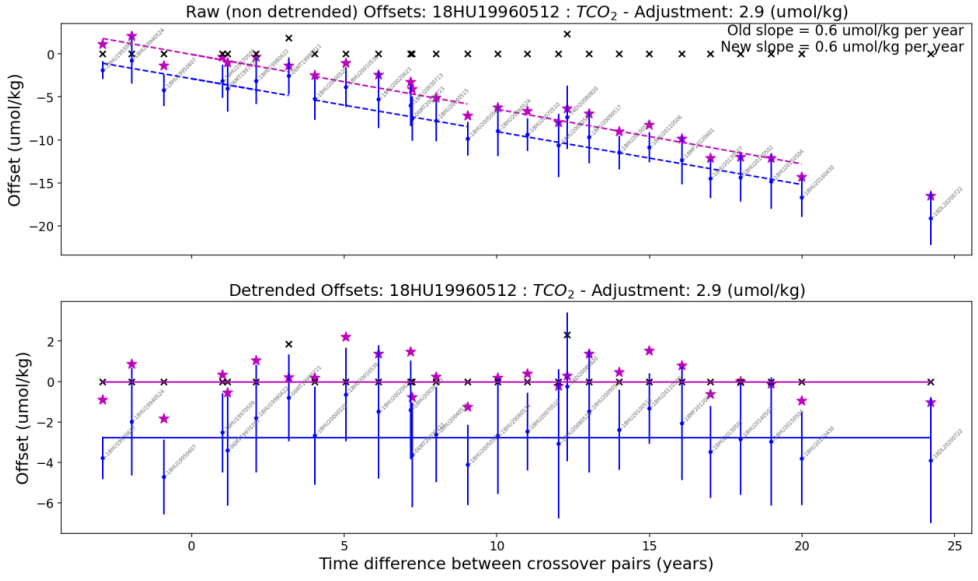

Figure 7: (a) The cruise-pair offsets (y-axis) for TCO_2 on cruise 18HU19960512 plotted against time (x-axis). Blue dots and error bars indicate the initial cruise-pair offset and standard deviation, while the pink stars indicate cruise-pair offset after the suggested adjustments (black crosses) have been applied to all other cruises in the cruise-pairs. Lines indicate the trend shown in the upper left corner. (b) Same as (a) but for the detrended cruise-pair offsets.

2.2.5 Secondary QC of Transient Tracers and delC13

In contrast to the other core parameters, the secondary QC of the transient tracers rarely relies on surrounding cruises, i.e., it is independent of the newly added cruises to the product. Instead, it relies on the inspection of surface saturation distributions and tracer-tracer relationships. Here transient tracers are CFC-11, CFC-12, CFC-113, CCl_4, and SF_6. For all, except for SF_6, an adjustment threshold of 5% is used (Olsen et al., 2016). For SF_6, a higher adjustment threshold of 10% is applied (Lauvset et al., 2022), as SF_6 is evaluated primarily through consistency with expected ranges using CFC-12 as a benchmark. Surface saturation plots were used to assess whether near-surface concentrations were physically consistent with expected atmospheric equilibrium conditions, which are regionally defined and not always 100%, while tracer ratio analyses provided an additional diagnostic of internal consistency at depths. Moreover, consistency among the different variables is taken into account, while appreciating that they have different atmospheric histories (Lauvset et al., 2023, Fig. 6). Consequently, there is no need to re-evaluate cruises included in earlier versions of GLODAP and only the five newly added cruises with transient tracer data were evaluated in detail for GLODAPv3. The previously established adjustments from GLODAPv2.2023 were retained for all other cruises (360 cruises). Note that negative transient tracer concentrations are typically associated with low tracer levels near the analytical detection limit and can arise from blank subtraction. Although such values are not suitable for use in analysis, they were retained in the dataset to avoid introducing a positive bias through skewed removal of low-end values.

For cruises that measured delC13 (in total 119), a thorough secondary QC has never been performed as part of GLODAP, and this is also true for GLODAPv3. However, derived adjustments based on a crossover assessment performed by Becker et al., (2016) are adopted for 24 cruises with deep delC13 data.

2.2.6 Uncertainties

Uncertainty can be thought of as “a variable associated with a value that permits a statement of the dispersion (interval) of reasonable values of the quantity measured, together with a statement of the confidence that the (true) value lies within the stated interval” (Newton et al. 2015).

https://doi.org/10.5194/essd-2026-496
Preprint. Discussion started: 31 July 2026

Open Access Earth System Science Data Discussions

While GLODAP is scrupulous about its treatment of measurement consistency between cruises, its secondary quality control methods do not directly speak to or quantify the true values of the quantities measured. The GLODAP methods therefore cannot fully quantify uncertainty. However, addressing a common user request, GLODAPv3 now provides more information about components of the uncertainty in the measured values in the product.

Similar to the approach of Carter et al. (2024), we separate uncertainty into components: $u_{\text{repeatability}}$ reflecting a component of uncertainty that is independent for every measurement, originating from variations in measurement practices between measurements on a cruise; u_{cruise} reflecting uncertainties from variations in practices that are consistent on a cruise but vary between cruises; and $u_{\text{calibration}}$ reflecting uncertainties that are inherent to the metrology and calibration approach. Separately for the core variables, GLODAPv3 now estimates and provides u_{cruise} for each cruise and $u_{\text{repeatability}}$ for the whole data product. GLODAPv3 does not attempt to quantify $u_{\text{calibration}}$.

The $u_{\text{repeatability}}$ values are given in Table 6 and represent target precision values based on recommended measurement practices and commonly reported repeatability estimates. These values should be regarded as performance targets rather than estimates achieved on every cruise. No attempt is made to provide this information on a cruise-by-cruise basis because repeatability estimates are inconsistently determined and reported across the cruises and variables in the data product.

The u_{cruise} estimates are derived from a consideration of the limits in our confidence in the adjustment procedure (i.e., minimum adjustment limits, Table 6) and the remaining inconsistencies of each cruise in the adjusted data product with respect to the other cruises in the adjusted data product. This is estimated as the sum in quadrature of the minimum adjustment limits (A_{min}) and the standard error (σ) on the CWMO ($\bar{\chi}$) that remains after adjustments are applied.

$$u_{cruise} = \sqrt{A_{min}^2 + \sigma_{\bar{x}}^2} \qquad (2)$$

For cruises without crossovers, twice the maximum standard error of the CWMO after adjustment observed among all other cruises is applied. For the Arctic, the standard error of the CWMO is replaced by the standard deviation of sub-basin-wide (adjusted) deep-water averages, and for transient tracers u_{cruise} was approximated by their minimum adjustment limits alone.

To propagate both $u_{\text{repeatability}}$ and u_{cruise} through a given analysis, we stress that these uncertainty components operate at different hierarchical levels, and that they must be represented separately within any error propagation framework. Specifically, $u_{\text{repeatability}}$ should be represented by independent perturbations applied to individual measurements, whereas u_{cruise} should be represented by a common perturbation affecting all measurements from a given cruise.

2.2.7 Merging Routine

The merging routine is a slightly modified version of the Make-Ocean routine used for previous GLODAP updates (Olsen et al., 2021), as visualized in Fig. 8. In brief, the routine merges individual cruise data by applying the following operations: selecting only good data (Table 3); merging bottle and CTD measurements for salinity and oxygen (Sect. 2.2.2); vertically interpolating temperature, salinity, oxygen, and macronutrient data; standardizing pH_T and fCO_2 data; applying the inversion-derived adjustments to the cruise data; calculating and assigning total cruise uncertainties (Sect. 2.2.6); and assigning corresponding quality flags (Table 5). Notably, the routine has been updated to generate additional columns for calculated carbonate system variables instead of merging measured and calculated carbonate system data in one column. The carbonate system is calculated using CO2SYSv3 with the set of constants described in Sect. 2.2.3. For calculations of TAlk or TCO_2, only pH_T data were used, and fCO_2 data were not considered. The final data product is provided as one global file and four regional (Arctic, Atlantic, Indian, Pacific) files in .csv, .mat. and netCDF format. For further details on the Make Ocean Routine, we refer the reader to Olsen et al., 2021 and Github (https://github.com/GLODAP/glodap.github.io, last accessed 26.06.2026).

https://doi.org/10.5194/essd-2026-496
Preprint. Discussion started: 31 July 2026

Open Access Earth System Science Data Discussions

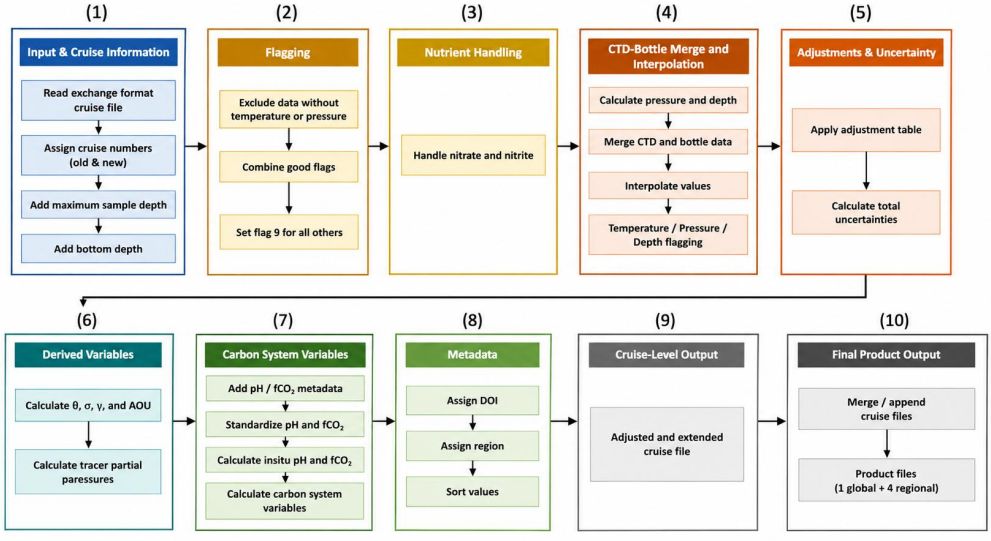

Figure 8: Flow chart displaying the updated MakeOcean Routine applied to generate the GLODAPv3 data products.

https://doi.org/10.5194/essd-2026-496
Preprint. Discussion started: 31 July 2026

3. Results and Adjustments

3.1 Trend preservation

While using only deep ocean data to identify potential offsets between cruises we cannot ignore the fact that human CO_2 emissions and climate change are regionally altering many of the GLODAP core variables at all ocean depths (e.g., Olsen et al., 2024). For GLODAPv3 we have made an additional effort to preserve such anthropogenic trends, the results of which are shown in Fig. 9. Since trends are estimated using cruise-pair offsets, which represent systematic differences between cruises, the trend detection method will inevitably lead to some dubious trends. It is therefore expected that some trends will be removed by the adjustment process. That this happens indeed is seen in Fig. 9 where several cruises have a zero-trend after adjustment (y-axes). In addition, as also seen in Fig. 9, the adjustment process introduces a trend in some cases. Generally, however, the applied adjustments do not alter the identified trends strongly, and trends identified for adjusted data are consistent with current knowledge on ocean changes (Talley et al., 2016; McDonagh et al., in press). We do indeed expect TCO_2 and oxygen, driven by increased anthropogenic carbon and deoxygenation, respectively, to exhibit trends in the deep ocean, and these are nicely preserved by our routine (Fig. 9). The largest trends in TCO_2 are up to 0.6 µmol $kg^{-1}year^{-1}$ and in oxygen -0.3 % $year^{-1}$. For silicate most of the initially identified trends are removed or strongly reduced (Fig. 9d). Likely, this is the result of a combination of relatively small initial trends with a higher standard deviation in the unadjusted CWMOs (4.4%) for silicate than in other macronutrients. The fact that pre-inversion adjustments are used to remove some systematic offsets in Japanese data (Sect. 3.2.4) may also contribute. We believe the same is the case for alkalinity, where pre-inversion adjustments likely contribute to the removal of spurious trends (Fig. 9b).

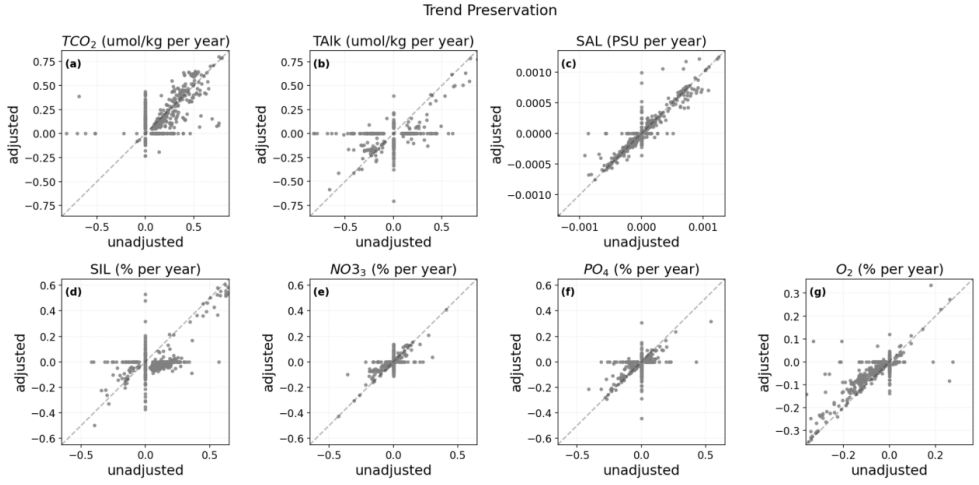

Figure 9: Per cruise trends in cruise-pair offsets before (x-axis) and after adjustments (y-axis) have been applied. The figure only shows trends that are significant as described in Sect. 2.2.4.2. The TCO_2 and TAlk trends are given in µmol kg^{-1} $year^{-1}$, salinity in $year^{-1}$ and the nutrients and oxygen in % $year^{-1}$.

3.2 Overview of secondary QC results

Data from a total of 1181 cruises were subject to secondary QC. However, since some cruises were split following the breakpoint analysis (see Sect. 2.2.4.1) or represent multiple cruises from a single campaign (e.g., TTO-NAS, Brewer et al., 2002), we have a total of 1224 entries (Table S1). To acknowledge this distinction, we will refer to entries rather than cruises in the next sections. A summary of the secondary QC actions are presented in Table 8, and Fig. 10 shows the distribution of the adjustments for the different decades. Additionally, Table 7 provides an overview of the implemented regional threshold values used for determining the 'Cruises-to-Adjust' list (Sect. 2.2.4.2). The regional thresholds show that adjustments are generally more robust (higher normalized adjustment thresholds) in the Pacific and less robust (lower normalized adjustment thresholds) in the Northern North Atlantic and Southern Ocean. The northern North Atlantic and Southern Ocean are the ocean regions where the deep ocean is most likely to exhibit both large natural variability and significant anthropogenic trends since the ocean mixes

https://doi.org/10.5194/essd-2026-496
Preprint. Discussion started: 31 July 2026

very deeply in these regions. It is thus only natural that the adjustments inferred from deep ocean crossovers have lower confidence in these regions.

Improvements in consistency are assessed using the weighted root mean squared error (wRMSE) and standard deviation across all CWMOs (Fig. 11) for the adjusted vs unadjusted data. The wRMSE is calculated as

$$wRMSE = \sqrt{\frac{\sum_i w_i \bar{x}_i^2}{\sum_i w_i}}, \text{ with } w_i = \frac{1}{u_{pre,i}^2} \qquad (3)$$

where the weights, w, are defined using the unadjusted CWMO standard errors, u_{pre}. These weights are held fixed when evaluating both the pre- and post-adjustment CWMOs to ensure consistency in the diagnostic metric. The wRMSE therefore quantifies the deviation of CWMO values from zero, corresponding to perfect 'cruise-level' consistency in the crossover network. The standard deviation provides a measure of the spread of CWMO values across cruises. For both metrics, a reduction indicates improved consistency. The average of all CWMO standard errors (Humphreys et al., 2026) is used as an additional diagnostic reflecting the level of confidence in the CWMO estimates. Thus, global consistency improves if both the wRMSE and the standard deviation of CWMOs decrease, while a concurrent reduction in the mean CWMO standard errors indicates a better constrained crossover network.

Table 8: Summary of secondary QC actions per variable for the 1224 entries.

	SAL	O_2	NO_3	SIL	PO_4	TCO_2	TAlk	CFC_11	CFC_12	CFC_113	SF_6	CCL_4	C13
No Data	1	90	128	161	153	230	373	892	864	1102	1127	1148	1090
With data	1223	1134	1096	1063	1071	994	851	332	360	122	97	76	134
Unadjusted	703	564	596	342	534	445	317	267	297	69	81	34	16
Adjusted	158	271	173	459	203	162	250	29	25	7	6	5	8
-888	356	278	294	228	284	353	249	30	29	23	8	16	109
-777	6	21	33	34	50	34	35	6	9	23	2	21	1

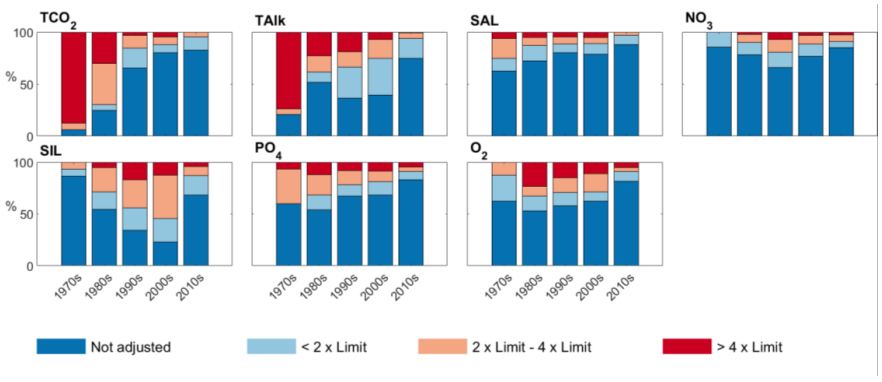

Figure 10: Distribution of applied adjustments per decade; Dark blue - not adjusted; Light blue - adjustment < minimum; Orange - adjustment between limit and 2 times limit, Red - adjustment > 2 times limit.

https://doi.org/10.5194/essd-2026-496
Preprint. Discussion started: 31 July 2026

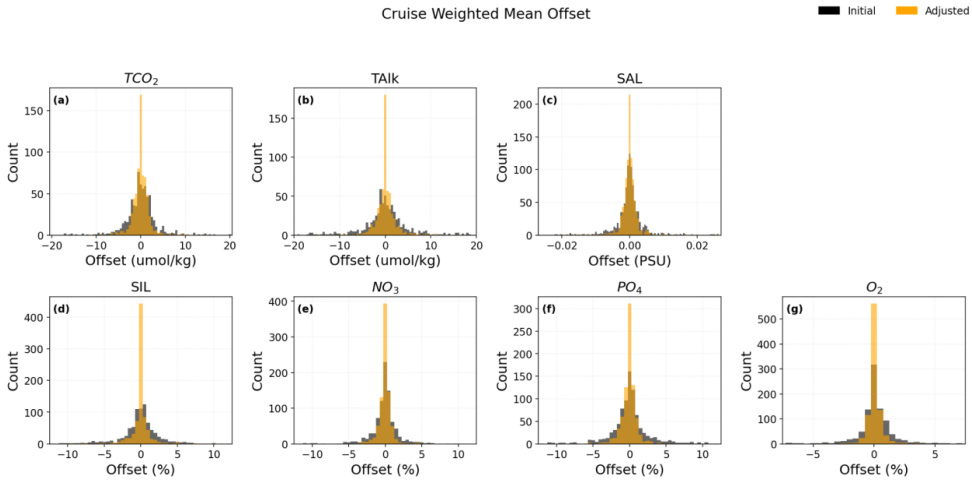

Figure 11: Fully global entry weighted mean offsets (CWMO) before (dark grey) and after (orange) adjustments being applied for all core variables except the halogenated transient tracers. Note that where they overlap the orange color appears darker so as to show the dark grey behind. The y-axis shows the number of cruises while the x-axis shows the CWMO.

Table 9: Global key improvement metrics per variable for the 1224 entries: weighted Root Mean Squared Error (CWMO wRMSE); the standard deviation of all CWMOs (CWMO Spread); and the average standard errors of all CWMOs (CWMO Uncertainty).

	CWMO wRMSE			CWMO Spread			CWMO Uncertainty		
	init		adj	init		adj	init		adj
SAL (ppm)	1.9	-->	1.3	6.1	-->	5.3	1.9	-->	1.7
O_2 (%)	0.7	-->	0.7	1.9	-->	0.9	0.5	-->	0.3
NO_3 (%)	0.7	-->	0.4	2.5	-->	1.0	0.6	-->	0.3
SIL (%)	1.5	-->	0.5	4.4	-->	2.6	1.2	-->	0.7
PO_4 (%)	1.1	-->	0.5	3.4	-->	1.4	0.9	-->	0.4
TCO_2 (µmol kg^{-1})	3.2	-->	1.2	5.2	-->	2.0	1.6	-->	0.8
TAlk (µmol kg^{-1})	4.8	-->	1.4	6.2	-->	2.6	1.8	-->	0.9

3.2.1 Temperature

No temperature adjustments have been applied. This decision reflects both the generally high internal consistency of temperature measurements and the limited applicability of the crossover analysis and inversion framework to temperature data. Even below 1500 dbar, spatial temperature gradients are several orders of magnitude larger than the systematic offsets targeted by the adjustment procedure. While more specialized quality-control approaches tailored specifically to temperature exist (e.g., Good et al., 2023), these are outside the scope of the secondary QC framework applied within GLODAP. Nevertheless, the analyses conducted here did not reveal any physically implausible temperature offsets between cruises. Note that all non-temperature data are removed when temperature data are missing.

3.2.2 Salinity adjustment summary

1223 entries have salinity data (Table 8). Note that all non-salinity data are retained even when salinity data are missing. Prior to the secondary QC, the CTD and bottle data were merged as summarized in Table 4. Data from 6

https://doi.org/10.5194/essd-2026-496
Preprint. Discussion started: 31 July 2026

entries were deemed too poor in quality for inclusion in GLODAPv3 (Table 8). Typically, these showed large and depth-dependent offsets and/or unrealistic scatter compared to background data. For 356 of the entries, secondary QC could not be carried out and of the remaining 861 entries, the salinity data from 152 were found to merit adjustment. Most of the (absolute) adjustments applied are between 0.0033 and 0.0079 (Fig. 10), with the largest negative and positive adjustments applied being -0.0342 and 0.0231. Application of the adjustments increased the overall consistency with a reduction of the wRSME from 0.0019 to 0.0013 and reduced the CWMO spread from 0.0061 to 0.0053 (Fig. 11; Table 9).

3.2.3 Oxygen adjustment summary

1136 entries have oxygen data (Table 8). Prior to the secondary QC, the CTD and bottle data were merged as summarized in Table 4. Data from 16 entries were deemed too poor in quality for inclusion in GLODAPv3 (Table 8) and for 288 of the entries, secondary QC could not be carried out. Of the remaining 832 entries, the oxygen data from 268 were found to merit adjustment. Most of the (absolute) adjustments applied are between 0.9 % and 2.1 % (Fig. 10), with the largest negative and positive adjustments applied being -9.7 % and 11.0 %. Even though the wRMSE increased slightly by 0.17 %, the application of the adjustments increased the overall consistency as shown by the decrease in CWMO spread (Fig. 11; Table 9).

3.2.4 Silicate adjustment summary

Silicate data were available for 1068 entries (Table 8). The silicate data from 34 entries were identified as being of insufficient quality, exhibiting excessive scatter, large offsets, drift, or a combination of these issues. Freezing of samples with silicate concentrations above approximately 50 µmol kg^{-1} was frequently identified as a cause of poor data quality, as freezing can decrease measured concentrations through polymerization (Becker et al., 2019). For 292 entries, secondary QC could not be carried out. Of the remaining 742 entries, silicate data from 401 were identified as requiring adjustment. This corresponds to almost 55 % of the entries, making silicate the most frequently adjusted variable in GLODAPv3. This high adjustment frequency is primarily due to the bulk pre-inversion adjustments applied to a large fraction of the Japanese entries, as well as all LineP entries.

For the Japanese pre-inversion adjustments, dedicated Japanese-only crossover and inversion analyses revealed systematic time-dependent offsets within the Japanese silicate data. As indicated by the suggested adjustments shown in Fig. 12a, Japanese silicate measurements obtained prior to 2010 tend to be approximately 2 % lower than those collected between 2010 and 2018, whereas post-2018 data are approximately 1 % higher relative to the 2010–2018 period. These small systematic offsets are only detectable due to the high precision of the Japanese data.

Almost all of the Japanese silicate data showing these systematic offsets come from the Japan Meteorological Agency (JMA), while data from JAMSTEC data may also contribute to the observed offsets, but to a lesser extent due to the smaller number of data. These intra-Japanese time-dependent offsets reflect systematic inconsistencies in analytical standardization. Within JMA, nutrients are primarily measured aboard the Research vessels R/V Ryofu Maru (49RY and 49UP) and R/V Keifu Maru (49UF), whereas JAMSTEC measurements are mainly conducted aboard the R/V Mirai (49NZ). The silicate measurements performed by JMA were consistently standardized using Merck silicon standard solutions traceable to NIST Standard Reference Materials. The pronounced offset identified around 2010 coincides with a change in the Merck standard solution lot (from HC814662 to HC074650). An approximately 2.5 % difference was observed between these lots, exceeding the manufacturer-stated uncertainty of 0.5 %. A similar change occurred around 2018, however, the associated difference remained within the stated uncertainty range of the standard solution. Also note that since 2019, JAMSTEC has used KANSO silicon standard solutions traceable to certified reference materials assigned by the National Metrology Institute of Japan.

Additional crossover and inversion analyses restricted to US and Japanese data collected between 2010 and 2018 (Fig. 12b) indicate no systematic offsets between these datasets. As a result, bulk pre-inversion adjustments were applied to the pre-2010 and post-2018 Japanese data in order to remove the intra-Japanese systematic offsets.

For the LineP pre-inversion adjustments, similar dedicated crossover and inversion analyses were performed (Fig. 13). Following the same rationale applied to the Japanese pre-inversion adjustments, these analyses supported a 1.5 % upward bulk adjustment for all LineP data, all of which were analyzed at the Institute of Ocean Sciences (Canada). In this case, however, no additional information could be obtained regarding the origin of the observed systematic offset.

https://doi.org/10.5194/essd-2026-496
Preprint. Discussion started: 31 July 2026

Following the application of the pre-inversion adjustments, all silicate data were subjected to the regular crossover and inversion analyses (Sect. 2.2.4). The applied adjustments substantially improved the global consistency of the silicate dataset, as demonstrated by reductions in both the wRMSE and the spread of the CWMOs (Fig. 11; Table 9). Note that samples analyzed ashore were more likely to require adjustment than samples analyzed onboard, reflecting the challenges associated with sample storage procedures.

Figure 12: Bulk pre-inversion adjustments for Japanese silicate data. Note that very large offsets were corrected before running the FF routine to avoid skewing the results. (a) Outcome of an inversion of only Japanese data; (b) Outcome of an inversion of only US data (orange), and only Japanese data post 2010 (black).

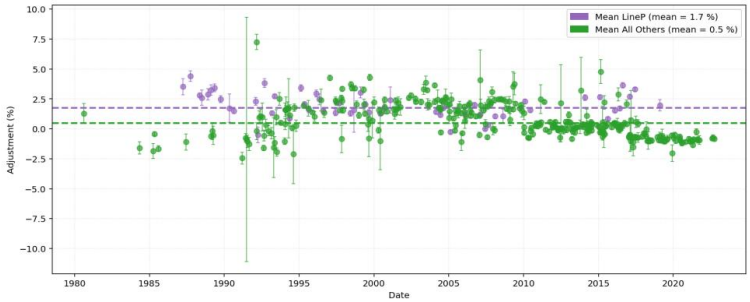

Figure 13: Bulk pre-inversion adjustments for silicate data on Line P. Note that very large offsets were corrected before running the FF routine to avoid skewing the results.

3.2.5 Phosphate adjustment summary

1074 entries came with phosphate data (Table 8). Data from 50 entries were deemed to be of too poor a quality for inclusion in GLODAPv3 and for 286 of the entries, secondary QC could not be carried out. Of the remaining 738 entries, the phosphate data from 201 were found to merit adjustment. Most of the (absolute) adjustments applied are between 1.6 % and 4.2 % (Fig. 10), with the largest negative and positive adjustments applied being -12.0 % and 13.9 %. Application of the adjustments increased the overall consistency of the data with a reduction of the wRSME from 1.1 % to 0.5 % and reduced the CWMO spread from 3.4 % to 1.4 % (Fig. 11; Table 9).

https://doi.org/10.5194/essd-2026-496
Preprint. Discussion started: 31 July 2026

3.2.6 Nitrate adjustment summary

1099 entries came with nitrate data (Table 8). Data from 32 entries were deemed to be of too poor a quality for inclusion in GLODAPv3 and for 298 of the entries, secondary QC could not be carried out. Of the remaining 769 entries, the nitrate data from 178 were found to merit adjustment. The bulk of the (absolute) adjustments applied are between 1.3 % and 3.1 % (Fig. 10), with the largest negative and positive adjustments applied being -6.0 % and 15.0 %. Application of the adjustments increased the overall consistency of the data with a reduction of the wRSME from 0.7 % to 0.4 % and reduced the CWMO spread from 2.5 % to 1.0 % (Fig. 11; Table 9).

3.2.7 TCO_2 adjustment summary

998 entries have TCO_2 data (Table 8). Data from 29 entries were deemed to be of too poor a quality for inclusion in GLODAPv3 and for 368 of the entries, secondary QC could not be carried out. Of the remaining 601 entries, the TCO_2 data from 158 were found to merit adjustment. Most of the absolute adjustments applied are between 2.6 µmol kg^{-1} and 6.4 µmol kg^{-1} (Fig. 10), with the largest negative and positive adjustments applied being -36.3 µmol kg^{-1} and 23.2 µmol kg^{-1}. Application of the adjustments increased the overall consistency of the data with a reduction of the wRSME from 3.2 µmol kg^{-1} to 1.2 µmol kg^{-1} and reduced the CWMO spread from 5.2 µmol kg^{-1} to 2.0 µmol kg^{-1} (Fig. 11; Table 9). Also note the decrease of adjustments over time (Fig. 10), coinciding with the broad application of standard operating procedures and introduction and common use of certified reference materials.

3.2.8 TAlk adjustment summary

998 entries have TAlk data (Table 8). Data from 30 entries were deemed to be of too poor a quality for inclusion in GLODAPv3 and for 282 of the entries, secondary QC could not be carried out. Of the remaining 544 entries, the TAlk data from 230 were found to merit adjustment. Thus, TAlk is the second most frequently adjusted variable in GLODAPv3. This reflects a systematic offset identified within Japanese Pacific cruises. A dedicated crossover and inversion analysis only including Japanese data indicated that pre-2010 Japanese entries are approximately 3 µmol kg^{-1} lower than post-2010 Japanese entries (Fig. 14a). Note that while the split coincides well with the onset of regular spectrophotometric alkalinity measurements by JMA in 2010, it is less consistent with the onset of regular spectrophotometric alkalinity measurements at JAMSTEC in 2007. Moreover, Woosley et al. (2025) concluded that a systematic alkalinity offset did not arise from methodological differences between single-point titration with spectrophotometric endpoint detection and potentiometric techniques. To gain better insight, additional crossover and inversion analyses including US data and only pre (post) 2010 Japanese data were performed (Fig. 14b). These indicated a good fit between post-2010 Japanese and US data. Although no definitive cause has been identified for this shift, we are more confident that the post-2010 Japanese data are accurate. Accordingly, all pre-2010 Japanese data received a 3 µmol kg^{-1} upward pre-inversion adjustment.

Following the application of the pre-inversion adjustments, all TAlk data were subjected to the regular crossover and inversion analyses (Sect. 2.2.4). The applied adjustments substantially improved the global consistency of the TAlk dataset, as demonstrated by reductions in both the wRMSE and the spread of the CWMOs (Fig. 11; Table 9). Also note the decrease of adjustments over time (Fig. 10), coinciding with the broad application of standard operating procedures and introduction and common use of certified reference materials.

https://doi.org/10.5194/essd-2026-496
Preprint. Discussion started: 31 July 2026

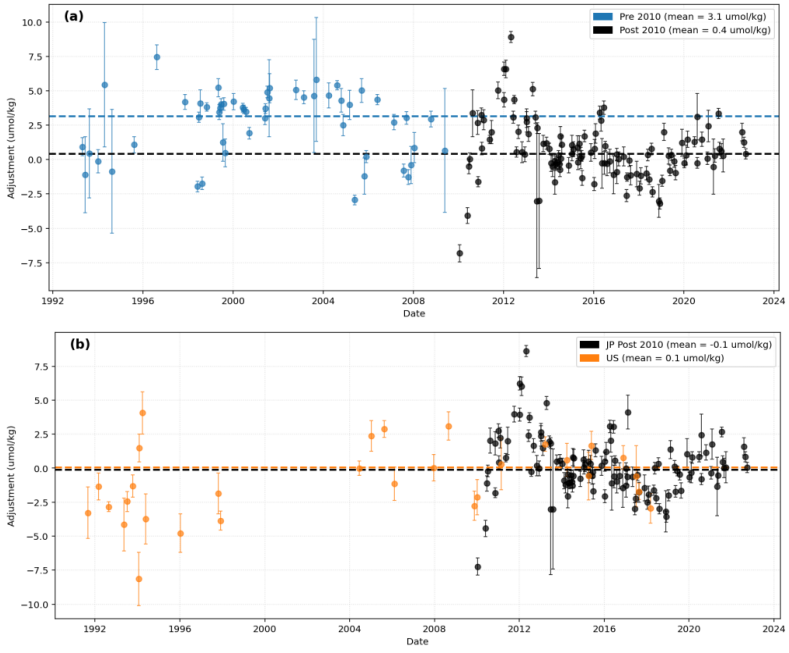

Figure 14: Bulk pre-inversion adjustments of Japanese alkalinity data. Note that very large offsets were corrected before running the FF routine to avoid skewing the results. (a) Outcome of an inversion of only Japanese data.; (b) Outcome of an inversion of only US data (orange), and Japanese data post 2010 (black).

3.2.9 Halogenated Tracers and SF_6

378 entries include data for at least one transient tracer (Table 8). While CFC-11 and CFC-12 were commonly measured during the WOCE and CLIVAR eras, SF_6 has become increasingly available in more recent decades, and CFC-113 and CCl_4 remain comparatively less frequently observed (Fig. 1). The adjustment summaries for halogenated transient tracers are based on cumulative secondary QC outcomes since GLODAPv2 (Sect. 2.2.5). The combination of spatially and temporally varying atmospheric equilibria and tracer concentration ranges in deep waters spanning approximately two orders of magnitude, make secondary QC particularly challenging. As a result, only a limited number of adjustments were applied overall.

For CFC-11 and CFC-12, six (nine) entries were deemed to be of too poor a quality for inclusion in GLODAPv3 (Table 8) and for 30 (29) entries, secondary QC could not be carried out. Of the remaining 267 (322) entries, the CFC data from 29 (25) were found to merit adjustment. The bulk of the adjustments applied are between -5 % (-5 %) and 5% (10 %) (Fig. 10).

For SF_6, two entries were deemed to be of too poor a quality (Table 8) and for 8 entries, secondary QC could not be carried out. Of the remaining 87 entries, the SF_6 data from 89 were found to merit adjustment. The bulk of the adjustments are between 10 % and 20 % (Fig. 10). While the saturation of CFC-12 was used as a benchmark for the magnitude of the adjustment, SF_6 was not adjusted to perfectly correlate with CFC-12, thereby preserving SF_6 as an independent constraint on ocean circulation.

For CFC-113 and CCl_4, 23 (21) entries were deemed to be of too poor a quality (Table 8) and for 23 (16) entries, secondary QC could not be carried out. Of the remaining 76 (39) entries, data from 7 (5) were found to merit adjustment. The bulk of the adjustments applied are between -2.5 % (-10 %) and 10 % (5 %) (Fig. 10). Adjustments were only applied where repeat cruises revealed clear and systematic inconsistencies in reported concentrations.

https://doi.org/10.5194/essd-2026-496
Preprint. Discussion started: 31 July 2026

Open Access Earth System Science Data Discussions

4. Discussion

4.1 pH data in GLODAPv3

As a major change in the methods employed in GLODAPv2 (including all the updates), secondary QC of pH_T was not carried out for GLODAPv3. Because there are relatively few cruises with pH data, the crossover and inversion methods were not used for pH_T in GLODAPv2. Instead pH_T was either corrected using internal consistency reasons as described by Olsen et al. (2016), or, for the updates, the number of pH_T crossovers was artificially increased by calculating pH_T from TCO_2 and TAlk in the adjusted reference dataset (i.e., GLODAPv2). Such calculations have uncertainties that are comparable to or only slightly worse than measurements (Millero, 2007), but the choice of dissociation constants and the boron/salinity ratio (Lee et al., 2010; Uppström, 1974) leads to subjective decisions with significant impacts on the resulting offsets (Fong & Dickson, 2019; Woosley, 2021; Woosley & Moon, 2023). Currently no consensus exists on which set of constants should be used (Carter et al., 2024b). In addition, the TAlk and TCO_2 pair for calculations has the largest uncertainty (McLaughlin et al., 2015; Millero, 2007), while discrete fCO_2 data are hardly available, and when combined with TCO_2 or TAlk to calculate pH_T, inconsistencies beyond uncertainty propagation are clearly identified (García-Ibáñez et al., 2022); additional complications derive from the possible presence of organic alkalinity, which is not considered in the calculations and could lead to a spurious offset that is due to uncertainties in TAlk rather than pH_T (Sharp & Byrne, 2020, 2021; Woosley et al., 2025). The conclusion from all such considerations is that using internal consistency between measured and calculated pH_T is inappropriate for secondary QC; consequently, few pH_T data were adjusted in the GLODAPv2 updates. For GLODAPv3 the state of knowledge was thoroughly reviewed. The decision not to apply secondary QC on pH_T data was primarily based on an improved understanding of pH_T uncertainties (Álvarez et al., 2020, 2025; Carter et al., 2024b; Carter et al., 2024a; Fong & Dickson, 2019; Pérez et al., 2026, Takeshita et al., 2021; Woosley & Moon, 2023), a growing recognition that a constant offset for each cruise was not appropriate (Carter et al., 2018; Takeshita et al., 2021; Woosley & Moon, 2023), and on challenges resulting from different methodologies.

Perhaps the biggest challenge in secondary QC of pH_T is the form that any adjustment should take. In GLODAPv2 constant offsets were used. However, since GLODAPv2 was first released, several studies have found that offsets are generally pH_T dependent (Álvarez et al., 2020; Carter et al., 2018; Carter et al., 2024a) and therefore adjustments should likely include a slope and intercept. Given the small dynamic range of pH_T in the deep-water reference layers, and the comparatively limited amount of pH_T measurements currently available, determining such offsets by crossovers alone would be highly uncertain at best. Recent studies suggest that using a constant offset based on deep-water reference layers may lead to an overcorrection of pH_T in surface waters (Williams et al., 2017; Álvarez et al., 2020; Pérez et al., 2026).

Although several measurement methods exist for many of the variables evaluated by GLODAP, pH_T methods have the most and the largest method-dependent potential offsets. These method-dependent differences are further exacerbated by the lack of a standard reference material for pH_T (Capitaine et al., 2023; Woosley et al., 2025). The two main methods for determining pH_T are potentiometry and spectrophotometry. Glass electrode potentiometric measurements are an order of magnitude less precise than spectrophotometric measurements and have mostly been determined to be of too low quality to be included in the GLODAP database (Olsen et al., 2016), so only few cruises were kept, the ones where primary QC showed low dispersion and reasonable accuracy. Yet, even with the very high precision of spectrophotometric pH_T, the discovery of impurities in the commercially available indicators used (Yao et al., 2007) and subsequent purification methods (Liu et al., 2011; Patsavas et al., 2013) leads to pH_T dependent offsets between measurements that used purified or unpurified indicator (Álvarez et al., 2020). Such differences can be accounted for (Douglas & Byrne, 2017) but the required corrections are rarely made, and accounting for impurities in historical data is difficult (Álvarez et al., 2025, Perez et al., 2026). Assuming that measurements using purified indicator represent the most accurate values currently available, it is possible to perform secondary QC using cruises with purified indicator as a reference; however, currently few such cruises (~40) are available and the global distribution is uneven. Further, efforts to account for methodological differences require a significant amount of metadata, which is often not available or difficult to find. The authors did attempt to compile such metadata, but it was extremely challenging and often the information is lacking in cruise reports or are unclear, particularly for older cruises. Given the ever-growing number of seawater pH_T measurements being made, however, and with concerted efforts to use purified indicators or account for impurities, it is possible to resolve these issues in future GLODAP versions. Doing so requires those that use purified indicator dye to verify the purity (Takeshita et al., 2021) and those using impure indicator dyes to account for impurities (Douglas & Byrne, 2017) and document how. Development of standard operating protocols and ensuring that laboratories

https://doi.org/10.5194/essd-2026-496
Preprint. Discussion started: 31 July 2026

make raw absorbance values publicly available would greatly improve the potential for secondary QC of pH_T in the future.

Globally, the uncertainty in pH_T is roughly comparable between GLODAPv2 and GLODAPv3, and there is no evidence of reduced quality of pH_T data in this latest version compared to previous versions. However, there are likely to be regional and cruise specific differences that should be evaluated when comparing studies that used different versions. Despite pH_T not receiving secondary QC in GLODAPv3, research to address the challenges discussed above combined with more measurements to increase the number of crossovers will likely allow pH_T to receive secondary QC in a future version.

4.2 Global vs Regional Consistency

The goal of GLODAP is to provide "an internally consistent biogeochemical data product of carbon-relevant data for the world ocean", by ensuring comparability among datasets to allow data sets from different sources to be used together with greater confidence. Achieving global consistency is not an easy task. It is well known that there are few cruises that connect the major ocean basins, and because those few cruises can strongly influence any global inversion solution for adjustments, GLODAP, following Gouretski and Jancke (2001) and Johnson et al. (2001), has historically relied on independent regional WLSQ inversions, where adjustments were determined separately within each individual ocean basin or even among groups of cruises in the same basin (Olsen et al., 2016). While this basin-specific framework effectively achieves basin-wide consistency, where adjustments roughly mirror initial CWMOs, it does not provide any information on global consistency. It should be added that in the context of GLODAP, consistency is not the same as accuracy. Even with broad access to certified reference materials for some variables (Aoyama et al., 2025), we cannot claim to know the accuracy of any ocean data since we do not know the true value.

With much more cruise data available than before for GLODAPv3, we tested whether a usable global consistency solution could be obtained. We compared the global WLSQ solution to basin-scale ones and found substantial differences. Further, a spatial pattern emerges when comparing the adjustment from the global WLSQ with the CWMOs (Fig. 15). Ideally the sum of these two should be zero, or very close to zero, but instead it tends to be negative in the northwest Pacific and positive elsewhere meaning that the northwest Pacific receives lower adjustments than expected from the CWMOs and all other regions receive higher than expected adjustments. While the spatial pattern differs somewhat across variables, all variables show similar large differences, with the most pronounced difference seen for TCO_2 (Fig. 15). Since there is no apparent physical or biogeochemical reason to expect systematic biases solely based on the cruises being in different ocean basins, there is reason to question the appropriateness of using this global solution to create a globally consistent data product. It appears that while the global WLSQ inversion gives us the mathematically optimal solution, it does not provide the optimal solution for GLODAP.

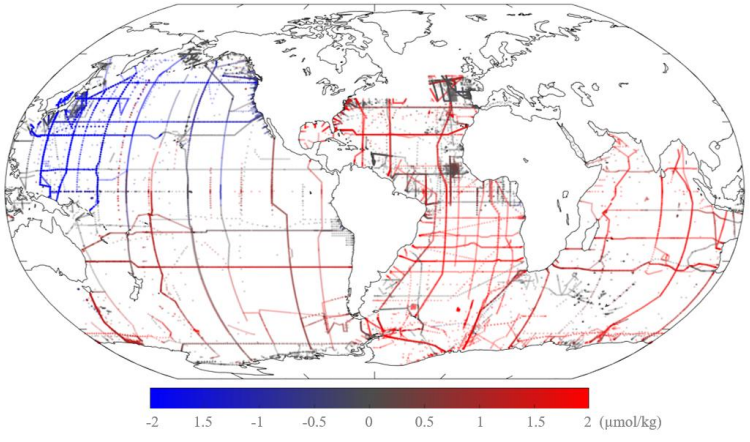

https://doi.org/10.5194/essd-2026-496
Preprint. Discussion started: 31 July 2026

Figure 15: Map showing the sum of the initial CWMO and the suggested adjustment from the global WLSQ solution. This example shows results from TCO_2 data in GLODAPv3. Note that the NNATL region and the Arctic is excluded from this inversion (see Sect. 2.2.4 for details).

To get a better understanding of these patterns, we performed a network analysis. Figure 16 illustrates the 'global' network for TCO_2 with nodes (shown as circles) representing each cruise (entry) and lines their connection, via cruise-pairs, to other cruises. Here, clusters of circles form whenever cruises are regionally well connected and spread out when there are fewer crossovers connecting collections of cruises. Generally, we see pronounced clustering with uneven cluster sizes and densities, as well as weak connectivity between the different clusters. The northwest Pacific represents the largest and densest cluster, reflecting the high repetition of a subset of cruises. Further, it is evident that the connection between the Pacific and Indian oceans is exceptionally weak (as indicated by the large yellow node in Fig. 16, corresponding to just a single cruise (49NZ20121128)), and that there is no direct connection at all between the Atlantic and Pacific oceans.

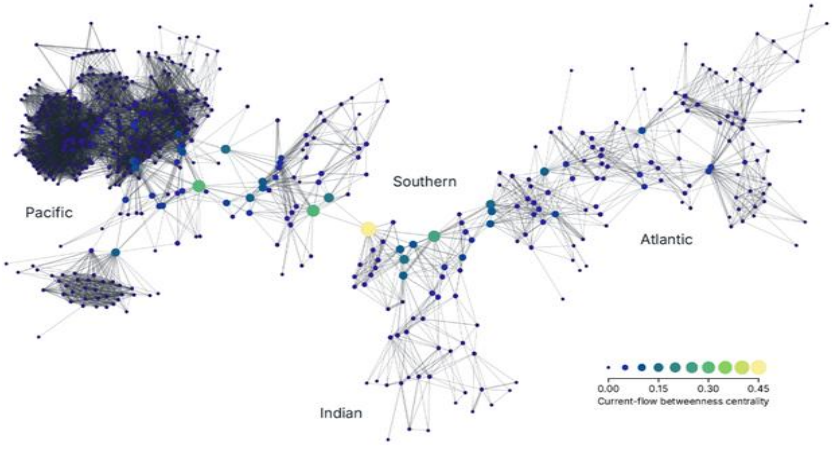

Figure 16: Cruise network for TCO_2 in GLODAPv3. Nodes (shown as circles) represent cruises and the lines their connection via cruise-pairs to other cruises. The size and color of the circles indicate the 'betweenness centrality' (Al-Ward et al., 2022), a metric indicating the importance of a node for connecting the network globally.

When iterated (~10^6 steps) to global convergence, i.e., steady state with respect to continuing iterations, the FF inversion approximates the same solution as the global WLSQ inversion (Humphreys et al., in prep). This highlights that it is the mathematically optimal solution to our matrix of equations. A great benefit of the FF inversion is that we can easily evaluate the adjustments at each iteration (Fig. 17), unlike the WLSQ which, from a user point of view, provides the solution in one step. In Fig. 17 each line represents the adjustments applied to a cruise at each iteration minus the final adjustment for that cruise after 10^6 iterations. The iterative process works in such a way as to maximize consistency between closely connected cruises first, meaning that clusters emerge. The colors in Fig. 17 indicate the cluster each region belongs to. These clusters are not pre-defined but emerge from the iterative adjustment process. As the iteration continues, the clusters are moved towards global consistency, using very small adjustments at each step. In the GLODAP network of cruises we find that global consistency is achieved by shifting all other clusters towards the Pacific Ocean cluster (PAC, Fig. 17), which is what we see in the WLSQ solution (Fig. 15).

By introducing a cut-off threshold within the FF inversion (step 2 as described in Sect. 2.2.4.2) we can stop the iterative process at the point where convergence within clusters is achieved. At this point all cruises in the Atlantic would need an additional upward adjustment of approximately 6 µmol kg^{-1} to converge with the Pacific, and all other regions 2-5 µmol kg^{-1}. We cannot think of any reasonable cause for such large adjustments and therefore

https://doi.org/10.5194/essd-2026-496
Preprint. Discussion started: 31 July 2026

choose to use the solution at the cut-off point. We want to note that Fig. 17 does not show that there is a 6 µmol kg⁻¹ difference between the Atlantic and Pacific in GLODAPv3. It merely shows that if allowed to run until full convergence the FF method would apply this, in our view incorrect and unnecessary, adjustment. Thus, although GLODAP aims to provide globally internally consistent data, the present analysis can only explicitly ensure regional internal consistency. Users of GLODAP should be aware of this important limitation. However, this does not imply that global consistency is absent. It rather indicates that the current characteristics of the global cruise-pair network, together with the uncertainties inherent in the crossover and inversion analysis, do not permit robust conclusions regarding global consistency.

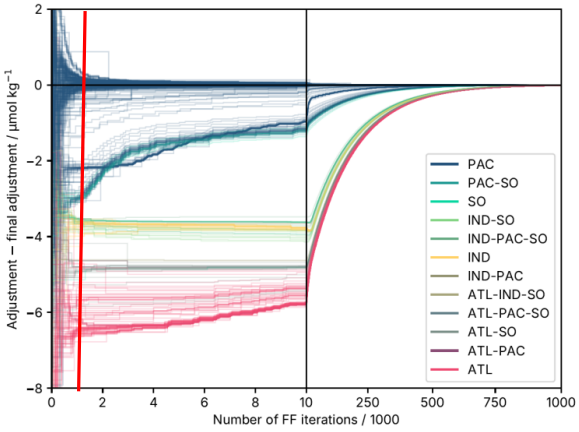

Figure 17: An example of how the iterative FF inversion works to create a globally convergent solution. The figure is created using the TCO_2 data in GLODAPv3. Each line represents the adjustments applied at a given iteration of the FF inversion minus the final adjustment after one million iterations. Colors indicate the cluster that each cruise belongs to. The vertical red line indicates the estimated cut-off (5% of the minimum adjustment limit), which for TCO_2 is iteration 1131. The vertical black line indicates a scale change of the x-axis.

4.3 Comparisons to GLODAPv2

Relative to GLODAPv2, the number of crossovers nearly doubled in GLODAPv3 (Table 10), underscoring the need for re-evaluation of all adjustments. Given this substantial increase in crossovers together with a more formalized method to retain trends in deep ocean data, statistically derived adjustment thresholds, and inversion solutions optimized for smaller regions, it is expected to see differences in the adjustments applied in GLODAPv3 relative to GLODAPv2 (including the updates). Figure 18 summarizes these differences. Overall, the mean and standard deviation of the differences are small and indicate no systematic shift. The large number of cruises that were unadjusted in GLODAPv2, but received adjustments in GLODAPv3 reflects the reduced minimum adjustment thresholds (Table 6). Conversely, cruises that were adjusted in GLODAPv2 but not in GLODAPv3 are mostly associated with adjustments that were large but too uncertain to justify correction.

The most substantial structural changes are present in silicate and alkalinity adjustments, a result of revised pre-inversion adjustments. In GLODAPv2 we were unable to find a definitive cause for the 2% systematic difference in silicate between Japanese and U.S. data (Fig. 5 in Olsen et al., 2016). As a pragmatic solution, Japanese data were therefore increased by 1% and U.S. data decreased by 1%. In the GLODAPv2 updates, new data were adjusted toward the reference dataset (Lauvset et al. 2022). With substantially more recent silicate data available for GLODAPv3, the 2% difference is now attributed to systematic inconsistencies within the Japanese data themselves (Fig. 11 and Fig. 12; Sect. 3.2.4), linked to changes in silicate standard solutions and to the uncertainty of the standard solutions. The resulting pre-inversion adjustments applied to pre-2010 and post-2019 Japanese data therefore constitute a major revision relative to GLODAPv2 and its updates. For alkalinity a systematic difference of 6 µmol kg⁻¹ between Japanese and U.S. cruises was identified in GLODAPv2 and corrected with a 6 µmol kg⁻¹

https://doi.org/10.5194/essd-2026-496
Preprint. Discussion started: 31 July 2026

pre-inversion adjustment for non-GO-SHIP Japanese data. However, this systematic difference could not be reproduced in the GLODAPv3 dataset. Instead, a systematic difference of 3 µmol kg^{-1} was identified between pre- and post-2010 Japanese data (Fig. 14; Sect. 3.2.8). While no definitive cause has been identified for this shift we are more confident that the post-2010 Japanese data are accurate since they align with alkalinity data from other countries. We therefore corrected the systematic difference in Japanese data by applying a bulk adjustment to all pre-2010 Japanese alkalinity data. This different pre-inversion adjustment relative to GLODAPv2 means that the pre-2010 Japanese alkalinity data in GLODAPv2 (and its updates) are ~3 µmol kg^{-1} higher than those same data in GLODAPv3. Noteworthy in this regard is Muller et al.'s (2023) additional 2.05 µmol kg^{-1} correction to post-2010 Japanese alkalinity data in GLODAPv2.2022 for their anthropogenic carbon estimates. Although that correction improved consistency, it effectively adjusted different decade(s) than are now adjusted in GLODAPv3.

The biggest structural difference between GLODAPv2 and GLODAPv3 is probably the approach to regionalize inversions. In GLODAPv2 the regions used in the WLSQ inversions were pre-defined, while in GLODAPv3 the clusters emerge directly from the iterative FF routine. In principle the regional solutions used in GLODAPv2 and the cluster convergence resulting in GLODAPv3 are the same, but the latter is a more objective approach to clustering based on the properties of the actual network of cruise-pairs, which also lead to a different number of clusters. The different clusters in GLODAPv2 versus GLODAPv3 also prevent a quantitative assessment of any differences in global (in)consistency in the two versions. Additional comparisons of the global consistency, i.e., the mean absolute error of all cruise-pair offsets after adjustments have been applied, between GLODAPv2 and GLODAPv3 indicate a general improvement for all core variables. Although the differences are modest, they likely reflect that there are more recent observations in GLODAPv3, and that recent observations benefit from improved methodologies and access to reference materials. We therefore conclude that despite the changes in methodology, we find no evidence of significant differences between GLODAPv2 and GLODAPv3 (aside from the bulk pre-inversion adjustments), but a slight improvement in the latter.

Table 10: Number of crossovers and in brackets number of cruises for the different cruise networks.

Parameter	Globe	NNATL	Arctic	Total
O_2	17006 (737)	2594 (123)	1388 (102)	20988
SAL	18378 (772)	3046 (135)	1618 (109)	23042
NO_3	15951 (689)	1275 (100)	1416 (102)	18642
PO_2	15204 (655)	928 (87)	1444 (102)	17576
SIL	13573 (653)	997 (101)	1407 (100)	15977
TCO_2	7170 (524)	924 (83)	788 (84)	8882
TAlk	5781 (473)	760 (74)	736 (80)	7277

https://doi.org/10.5194/essd-2026-496
Preprint. Discussion started: 31 July 2026

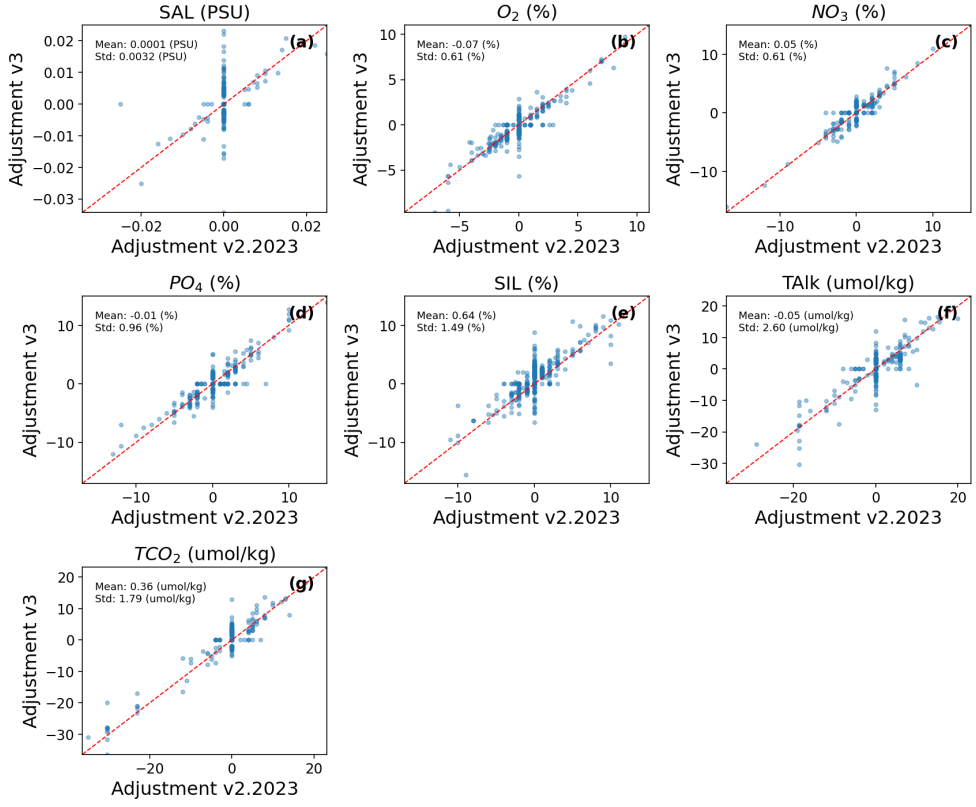

Figure 18: Applied adjustments in GLODAPv3 (y-axis) against the adjustments applied in GLODAPv2.2023 (x-axis). Mean and standard deviation of their difference shown as well.

https://doi.org/10.5194/essd-2026-496
Preprint. Discussion started: 31 July 2026

Open Access Earth System Science Data Discussions

5. Lessons learned and Outlook

5.1 Systematic metadata requirements

GLODAP has compiled a Metadata Table (https://github.com/GLODAP/glodap.github.io/tree/main/docs/MetaData, last accessed 26.06.2026) which is intended both as a living resource and as a foundation for more standardized and structured metadata reporting practices. Accordingly, the systematic examination of available cruise reports and additional metadata information to improve the transparency and usability of all (meta)data has been an ongoing effort within GLODAPv3. Where available, the compiled information includes the general analytical methods applied during each cruise, the instruments used, the pH and fCO_2 measurement scales and temperature conditions, as well as the use of (certified) reference materials ((C)RMs). Additional metadata fields document whether analyses were conducted on-board or on-shore after the cruise, as well as information related to sample preservation and storage. At present, about 75% of cruises have undergone this detailed metadata examination, and the effort is ongoing. However, it should be noted that detailed methodological metadata are frequently missing or incomplete, and discrepancies between cruise reports and the corresponding submitted data files are relatively frequent. In particular, whether and how (C)RM-based corrections are applied could not always be identified, which complicates the retrospective assessment of methodological biases and uncertainties.

5.2 Outlook

Several developments are planned to extend the functionality and scientific utility of GLODAP.

The most immediate planned addition to GLODAPv3 is the development of a mapped (gridded) version of the product, similar to that published by Lauvset et al. (2016) for GLODAPv2. For this, the Data-Interpolating Variational Analysis (DIVA) method (Beckers et al., 2014; Barth et al., 2014) will be applied to GLODAPv3 to provide global 1° × 1° mapped fields of temperature, salinity, oxygen, nutrients, inorganic carbon parameters, and water ages derived from halogenated transient tracers. Following a structure analogous to the World Ocean Atlas (Reagan et al., 2023), four climatologies will be generated: a 50-year average climatology covering 1972–2022, and three decadal climatologies for the 1990s, 2000s, and 2010s. All climatology products will be accompanied by corresponding uncertainty fields, propagating the observational uncertainties (Sect. 2.2.6) through the mapping procedure, and explicitly accounting for representation error (Gregor and Gruber, 2021).

Methodological expansion is also desired for GLODAP through the development of a dedicated data ingestion system, likely in collaboration with the autonomous CARIMED (Álvarez et al. 2025) that adds a significant number of cruises from the Mediterranean Sea, to streamline (meta) data integration and quality control workflows.

Despite these future ambitions, the GLODAP effort remains entirely dependent on project-based funding. This structural limitation poses challenges for long-term sustainability and capacity planning (Tanhua et al., 2021). In addition, a continued decrease in the number of available cruises since approximately 2015 represents an ongoing constraint, potentially affecting future data coverage and update frequency (Fig. 19). A similar decline in data availability has also been observed in SOCAT (Bakker et al., 2025). At the time of writing, continued updates of GLODAPv3, similar to those for GLODAPv2, have not been funded. It is nevertheless our ambition to release the first update in 2028, subject to available funding.

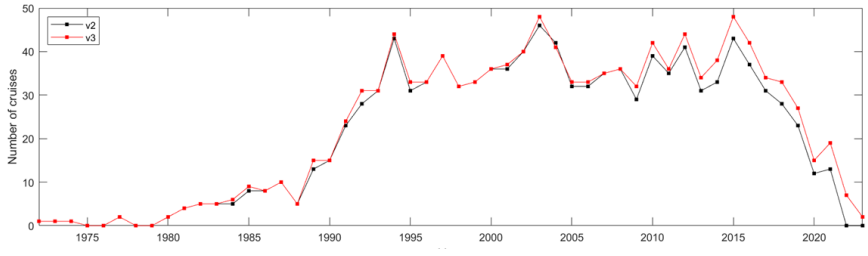

Figure 19.: Number of cruises per year in GLODAPv2.2023 (black) and GLODAPv3 (red).

https://doi.org/10.5194/essd-2026-496
Preprint. Discussion started: 31 July 2026

5.3 Recommendations

Based on the development of GLODAPv3, several recommendations can be made regarding its use, future data provision, and broader strategies for improving the cruise network.

Users of the data product should note that all data included in GLODAP are of high quality as a result of primary quality control. The secondary QC flag (Table 5) in turn only indicates whether systematic differences relative to other cruises could be assessed and corrected for. Data without secondary QC are thus not to be confused with poor-quality data. Further, the calculated carbon system variables (Sect. 2.2.7) are provided for convenience. However, depending on the scientific objective, recalculation of carbonate system variables using alternative equilibrium constants or a different combination of input variables, for example including fCO_2, may be preferable.

To further improve usability and interoperability of ocean biogeochemical data, we recommend more comprehensive and standardized metadata reporting practices together with the provision of metadata in structured, machine-readable formats. In particular, metadata should include information such as absorbance and measurement temperature data for spectrophotometric pH analyses, as well as explicit documentation of whether and how (C)RM-based corrections have been applied to variables such as TAlk, TCO_2 and the macronutrients. Similarly, improved synchronization across distributed data archives would strengthen consistency, and interoperability between different access points.

Based on the network analysis presented in Fig. 16, we further recommend the establishment of new cruise sections in regions that strengthen inter-basin connectivity and reduce dependence on a limited number of high-centrality crossover nodes. Theoretically, this could best be achieved through large-scale “super cruises” designed to intersect all regional clusters. However, given the substantial logistical and financial constraints associated with such expeditions, including ship time, fuel costs, and personnel availability, realization of this is unlikely in practice. Nevertheless, broader discussion within the seagoing oceanographic community on strategies to improve inter-cluster connectivity remains necessary.

Code and Data Availability

The merged and adjusted GLODAPv3 data product (https://doi.org/10.25921/m6tp-mj50) is archived at OCADS of NOAA NCEI under the CC BY 4.0 license. The data product is distributed as comma-separated ASCII files (*.*csv*), as Network Common Data Form files (*.*nc*), and as binary MATLAB (*.*mat*) files using the open-source Hierarchical Data Format Version 5 (HDF5). In addition, the product is available as an Ocean Data View (ODV) file that can be explored online through the “webODV Explore” service and via the Environmental Research Division’s Data Access Program (ERDDAP) server. As for GLODAPv2, regional subsets are provided for the Arctic, Atlantic, Pacific, and Indian oceans. These subsets do not overlap, and each cruise is assigned to only one basin file, even when cruise tracks extend across basin boundaries.

All figures and cruise statistics generated during the secondary QC procedures are available through the online GLODAPv3 Adjustment Table (https://glodapv3.geomar.de, last accessed 26.06.2026) hosted by GEOMAR, Kiel, Germany. The Adjustment Table follows the structure and functionality of the GLODAPv2 Adjustment Table (Olsen et al., 2016). Tables with all the GLODAPv3 cruise-pair offsets are provided through the GLODAP GitHub repository (https://github.com/GLODAP/glodap.github.io, last accessed 26.06.2026). The repository also contains all code used in the preparation of GLODAPv3, including a script for removing all applied adjustments and generating an unadjusted version of GLODAPv3 (reversing step 5 in Fig. 8). The GLODAPv3 Metadata Table (Sect. 5.1) is hosted here, as well.

The original cruise files are also publicly available and can be accessed via the DOIs provided within the data product. The files are distributed in WOCE exchange format (Sect. 2.2.1) and include updated WOCE flags, but do not include any adjustments, nor merged bottle and CTD values for oxygen and salinity. Note that, for some time series or campaigns, the data have not been segmented into individual cruises but instead maintained as collections under a single EXPOCODE (Table S1).

While GLODAPv3 is openly available without restrictions, users are encouraged to follow fair data use principles. Studies relying on specific cruise data should acknowledge the contributions of the original data providers by citing both the relevant cruise DOI(s) and associated publications describing the datasets. Users are also

https://doi.org/10.5194/essd-2026-496
Preprint. Discussion started: 31 July 2026

Open Access Earth System Science Data Discussions

encouraged to contact the principal investigators to discuss opportunities for collaboration and co-authorship. To this end, DOIs are included in the product files. Communication with the principal investigators can further improve scientific interpretation, as they often possess expert knowledge of the sampled regions and datasets. Proper citation of this paper in publications using the product is also encouraged, as citation tracking supports continued funding and future updates of GLODAP.

Author Contributions

Siv K. Lauvset, Brendan R. Carter, and Nico Lange led the team that produced GLODAP version 3. Siv K. Lauvset, Brendan R. Carter, Nico Lange, Matthew P. Humphreys, and Ryan J. Woosley created the original draft. Alex Kozyr compiled the original data files and maintains the GLODAPv3 web pages at NCEI/OCADS. Matthew P. Humphreys developed and coded the FF routine. Nico Lange conducted the primary and secondary QC analyses and generated the final product. Ryan J. Woosley led the pH working group. Carsten Schirnick manages the adjustment table e-infrastructure. Toste Tanhua, Reiner Steinfeldt, Emil Jeansson, and Nico Lange performed the secondary QC on all transient tracers. All authors contributed to the interpretation of the secondary QC results, made decisions on whether to apply (pre-inversion) adjustments, and contributed to writing the manuscript. Many authors contributed to final checks of the data product and conducted ancillary QC analyses.

Competing interests

At least one of the (co-)authors is a member of the editorial board of Earth System Science Data.

Disclaimer

Copernicus Publications adds a standard disclaimer: “Copernicus Publications remains neutral with regard to jurisdictional claims made in the text, published maps, institutional affiliations, or any other geographical representation in this paper. While Copernicus Publications makes every effort to include appropriate place names, the final responsibility lies with the authors. Views expressed in the text are those of the authors and do not necessarily reflect the views of the publisher.”

Acknowledgements

GLODAPv3 would not have been possible without the effort of the many scientists who secured funding, dedicated time to collect data, and shared the data that are included. The GLODAP team wants to especially thank Bob Key for his tireless effort to make sure the world has access to high-quality observational data on the global biogeochemical cycles. GLODAP version 3 only builds on the previous versions of GLODAP, and without Bob there would be no GLODAP. The author team also wants to thank the large GLODAP user community for useful input and notifications about potential issues in the data products. Such input is invaluable and helps ensure that GLODAP maintains its high quality and consistency over time. We also thank Tobias Ehmen and Houda Beghoura for thoroughly testing the GLODAPv3. This activity has been supported by the International Ocean Carbon Coordination Project (IOCCP), and the author team acknowledges funding to IOCCP provided by a grant to SCOR from the U.S. National Science Foundation (grant no. OCE-2513154).

Financial Support

Nico Lange, Siv K. Lauvset, and Are Olsen have received funding from the EU Horizon Europe project OceanICU (grant no. 101083922). Views and opinions expressed are however those of the author(s) only and do not necessarily reflect those of the European Union or European Research Executive Agency. Neither the European Union nor the granting authority can be held responsible for them. This publication is partially funded by the Cooperative Institute for Climate, Ocean, & Ecosystem Studies (CICOES) under National Oceanic and Atmospheric Administration (NOAA) Cooperative Agreement NA20OAR4320271, Contribution No.: 2026-1566. NOAA Pacific Marine Environmental Laboratory has assigned PMEL Contribution Number 5883. Brendan R. Carter is supported by the Carbon Data Management and Synthesis Project (Fund Ref. 100007298) of the Global Ocean Monitoring and Observing division of NOAA. Larissa Dias received support through OAR Climate Program Office (grant no. NA21OAR4310251) and the Global Ocean Monitoring and Observing program of NOAA through funding to the Carbon Data Management and Synthesis Program (grant no. 100007298). Ryan J.

https://doi.org/10.5194/essd-2026-496
Preprint. Discussion started: 31 July 2026

Woosley has been supported by NSF grants (grant nos. OCE-1923312 OCE-2148468and OCE-2342986). Alex Kozyr has been supported by NOAA (grant no. NA19NES4320002; Cooperative Institute for Satellite Earth System Studies – CISESS) at the University of Maryland/ESSIC. Leticia Cotrim da Cunha has been supported by the Prociencia 2025–2027 grant from Universidade do Estado do Rio de Janeiro (UERJ, Brazil) and the PQ-C 306250/2025-0 grant from the National Council for Scientific and Technological Development (CNPq, Brazil). Marta Álvarez has been supported by an Instituto Español de Oceanografía (IEO) RADPROF project. Peter J. Brown has received partial funding from the UK Climate Linked Atlantic Sector Science (CLASS) NERC National Capability Long-term Single Centre Science Programme (grant no. NE/R015953/1). Anton Velo and Fiz F. Perez have been supported by the BOCATS2 (grant no. PID2019-104279GB-C21) and by FICARAM+ (PID2023-148924OB-I00) projects funded by MCIN/AEI/10.13039/501100011033 and the Horizon Europe project EuroGO-SHIP (grant no. 101094690). Mario Hoppema has received funding from the EU Horizon 2020 Action SO-CHIC (grant no. 821001). Kumiko Azetsu-Scott acknowledges funding from Fisheries and Oceans Canada, including ACCASP, OFSI, and AZOMP. Jens D. Müller receives funding for a research fellowship through the Carbon to Sea initiative. Masao Ishii has been supported by the Environment Research and Technology Development Fund of the Environmental Restoration and Conservation Agency of Japan (grant no. JPMEERF24S12200). Susan Becker has been supported by NSF grant OCE 2023545.

https://doi.org/10.5194/essd-2026-496
Preprint. Discussion started: 31 July 2026

References

Álvarez, M., García-Ibáñez, M. I., Lange, N., Kozyr, A., Velo, A., Tanhua, T., Civitarese, G., Cantoni, C., Belgacem, M., Schroeder, K., Acerbi, R., Coppola, L., Wagener, T., Fajar, N. M., Flecha, S., Giani, M., Giannoudi, L., Guallart, E. F., Hassoun, A. E. R., Huertas, E. I., Ibello, V., Keraghel, M. A., Louanchi, F., Luchetta, A., Pérez, F. F., Schirnick, C., Souvermezoglou, E., Urbini, L., Vidal, M., and Ziveri, P.: CARIMED (CARbon, tracers, and ancillary data In the MEDiterranean Sea): A ship-based data synthesis product – overview and quality control procedures, Earth Syst. Sci. Data Discuss. [preprint], https://doi.org/10.5194/essd-2025-759, in review, 2025.

Álvarez, M., Fajar, N. M., Carter, B. R., Guallart, E. F., Pérez, F. F., Woosley, R. J., & Murata, A. (2020). Global ocean spectrophotometric pH assessment: consistent inconsistencies. *Environmental Science & Technology*, acs.est.9b06932. https://doi.org/10.1021/acs.est.9b06932

Álvarez, M., García-Ibáñez, M. I., Acerbi, R., Santiago-Domenech, R., Guallart, E. F., Fajar, N. M., & Arbilla, L. (2025). Ocean acidification at the crossroads I: Harmonizing unpurified and purified meta-cresol purple spectrophotometric pHT measurements based on absorbance data. *Limnology and Oceanography: Methods*. https://doi.org/10.1002/lom3.70023

Al-Ward, H., Tan, C. K., and Lim, W. H.: Caching transient data in Information-Centric Internet-of-Things (IC-IoT) networks: A survey, Journal of Network and Computer Applications, 206, 103491, https://doi.org/10.1016/j.jnca.2022.103491, 2022.

Aoyama, M., Cheong, C. and Murata, A. eds. (2025). Chemical Reference Materials for Oceanography: History, Production, and Certification. Singapore: Springer Nature. https://doi.org/10.1007/978-981-96-2520-8.

Bakker, Dorothee C. E.; Alin, Simone R.; Aramaki, Takafumi; Barbero, Leticia; Bates, Nicholas; Gkritzalis, Thanos; Jones, Steve D.; Kozyr, Alex; Lauvset, Siv K.; Macovei, Vlad A.; Metzl, Nicolas; Munro, David R.; Nakaoka, Shin-ichiro; O'Brien, Kevin M.; Olsen, Are; Pierrot, Denis; Steinhoff, Tobias; Sullivan, Kevin F.; Sutton, Adrienne J.; Sweeney, Colm; Wada, Chisato; Wanninkhof, Rik; Akl, John; Arbilla, Lisandro A.; Azetsu-Scott, Kumiko; Battisti, Roman; Beatty, Cory M.; Becker, Meike; Benoit-Cattin, Alice; Berghoff, Carla F.; Bittig, Henry C.; Bonin, Jennifer A.; Bott, Randy; Bozzano, Roberto; Burger, Eugene F.; Brunetti, Fabio; Cantoni, Carolina; Castelli, Giuliano; Chambers, Don P.; Chierici, Melissa; Corbo, Andrea; Cronin, Margot; Cross, Jessica N.; Currie, Kim I.; Dentico, Carlotta; Emerson, Steven R.; Enochs, Ian C.; Enright, Matt P.; Enyo, Kazutaka; Ericson, Ylva; Evans, Wiley; Fay, Amanda R.; Feely, Richard A.; Fragiacomo, Elena; Fransson, Agneta; Gehrung, Martina; Giani, Michele; Glockzin, Michael; Hamnca, Siyabulela; Holodkov, Nikola; Hoppema, Mario; Ibánhez, J. Severino P.; Kadono, Koji; Kamb, Linus; Kralj, Martina; Kristensin, Tor O.; Laudicella, V. Alessandro; Lefèvre, Nathalie; Leseurre, Coraline; Lo Monaco, Claire; Maenner Jones, Stacy; Maenza, Reinaldo A.; McAuliffe, Anna M.; Mdokwana, Baxolele; Monacci, Natalie M.; Musielewicz, Sylvia; Neill, Craig; Newberger, Tim; Nojiri, Yukihiro; Ohman, Mark D.; Ólafsdóttir, Sólveig R.; Olivier, Léa; Omar, Abdirahman M.; Osborne, John; Pensieri, Sara; Petersen, Wilhelm; Plueddemann, Albert J.; Rehder, Gregor; Roden, Nicholas P.; Rutgersson, Anna; Sallée, Jean-Baptiste; Sanders, Richard; Sarpe, Dick; Schirnik, Carsten; Schlitzer, Reiner; Send, Uwe; Skjelvan, Ingunn; Sutherland, Stewart, C.; T'Jampens, Michiel; Tamsitt, Veronica; Telszewski, Maciej; Theetaert, Hannelore; Tilbrook, Bronte; Trull, Tom; Tsanwani, Mutshutshu; Van de Velde, Sebastiaan; Van Heuven, Steven M. A. C.; Veccia, Martín H.; Voynova, Yoana G.; Weller, Robert A.; Williams, Nancy L. (2025). Surface Ocean CO2 Atlas Database Version 2025 (SOCATv2025) (NCEI Accession 0304549). NOAA National Centers for Environmental Information. Dataset. https://doi.org/10.25921/648f-fv35.

Barth, A., Beckers, J. M., Troupin, C., Alvera-Azcárate, A., and Vandenbulcke, L.: divand-1.0: n-dimensional variational data analysis for ocean observations, Geoscientific Model Development, 7, 225–241, 10.5194/gmd-7-225-2014, 2014.

Becker, M., Andersen, N., Erlenkeuser, H., Humphreys, M. P., Tanhua, T., and Körtzinger, A.: An internally consistent dataset of δ^{13}C-DIC in the North Atlantic Ocean – NAC13v1, Earth Syst. Sci. Data, 8, 559–570, https://doi.org/10.5194/essd-8-559-2016, 2016.

Beckers, J.-M., Barth, A., Troupin, C., and Alvera-Azcárate, A.: Approximate and Efficient Methods to Assess Error Fields in Spatial Gridding with Data Interpolating Variational Analysis (DIVA), Journal of Atmospheric and Oceanic Technology, 31, 515–530, 10.1175/JTECH-D-13-00130.1, 2014.

https://doi.org/10.5194/essd-2026-496
Preprint. Discussion started: 31 July 2026

Capitaine, G., Stoica, D., Wagener, T. and Fisicaro, P., 2023. Production of a reference material for seawater pHTmeasurements by a National Metrology Institute. Marine Chemistry, 252, p.104244. https://doi.org/10.1016/j.marchem.2023.104244.

Carter, B. R., Radich, J. A., Doyle, H. L., & Dickson, A. G. (2013). An automated system for spectrophotometric seawater pH measurements. *Limnology and Oceanography: Methods*, *11*(1), 16–27. https://doi.org/10.4319/lom.2013.11.16

Carter, B.R., Feely, R.A., Mecking, S., Cross, J.N., Macdonald, A.M., Siedlecki, S.A., Talley, L.D., Sabine, C.L., Millero, F.J., Reimer, J.J. and Takahashi, T. (2017). Two decades of bulk ocean acidification in the southwest Pacific Ocean along 170°W. Global Biogeochemical Cycles, 31(3), pp.562–587. https://doi.org/10.1002/2016GB005485.

Carter, B. R., Feely, R. A., Williams, N. L., Dickson, A. G., Fong, M. B., & Takeshita, Y. (2018). Updated methods for global locally interpolated estimation of alkalinity, pH, and nitrate. *Limnology and Oceanography: Methods*, *16*(2), 119–131. https://doi.org/10.1002/lom3.10232

Carter, B. R., Feely, R. A., Lauvset, S. K., Olsen, A., DeVries, T., & Sonnerup, R. (2021). Preformed properties for marine organic matter and carbonate mineral cycling quantification. Global Biogeochemical Cycles, 35, e2020GB006623. https://doi.org/10.1029/2020GB006623.

Carter, B. R., Sharp, J. D., García-Ibáñez, M. I., Woosley, R. J., Fong, M. B., Álvarez, M., et al. (2024a). Random and systematic uncertainty in ship-based seawater carbonate chemistry observations. *Limnology and Oceanography*, 1–16. https://doi.org/10.1002/lno.12674

Carter, B. R., Sharp, J. D., Dickson, A. G., Álvarez, M., Fong, M. B., García-Ibáñez, M. I., et al. (2024b). Uncertainty sources for measurable ocean carbonate chemistry variables. *Limnology and Oceanography*, *69*(1), 1–21. https://doi.org/10.1002/lno.12477

Clayton, T. D., & Byrne, R. H. (1993). Spectrophotometric seawater pH measurements : total hydrogen ion concentration scale calibration of m-cresol purple and at-sea results. *Deep-Sea Research I*, *40*(10), 2115–2129. https://doi.org/10.1016/0967-0637(93)90048-8

Dickson, A. G. (1990). Standard potential of the reaction: AgCl(S) + 12H2(g) = Ag(s) + HCl(aq), and the standard acidity constant of the ion HSO4- in synthetic sea water from 273.15 to 318.15 K. *The Journal of Chemical Thermodynamics*, *22*(2), 113–127. https://doi.org/10.1016/0021-9614(90)90074-Z

Doney, S. C., Balch, W. M., Fabry, V. J., and Feely, R. A.: Ocean Acidification: A critical emerging problem for the ocean sciences, Oceanography, 22, 16–25, 2009. https://doi.org/10.5670/oceanog.2009.93

Douglas, N. K., & Byrne, R. H. (2017). Achieving accurate spectrophotometric pH measurements using unpurified meta-cresol purple. *Marine Chemistry*, *190*, 66–72. https://doi.org/10.1016/J.MARCHEM.2017.02.004

Fasham, M.J.R., Baliño, B.M., Bowles, M.C., Anderson, R., Archer, D., Bathmann, U., Boyd, P., Buesseler, K., Burkill, P., Bychkov, A., Carlson, C., Chen, C.T.A., Doney, S., Ducklow, H., Emerson, S., Feely, R., Feldman, G., Hansell, D., Garçon, V. and Wong, C.S. (2001). A new vision of ocean biogeochemistry after a decade of the Joint Global Ocean Flux Study (JGOFS). Ambio, (Sp. Issue 10), pp.4–31.

Fong, M. B., & Dickson, A. G. (2019). Insights from GO-SHIP hydrography data into the thermodynamic consistency of CO2 system measurements in seawater. *Marine Chemistry*, *211*, 52–63. https://doi.org/10.1016/J.MARCHEM.2019.03.006

Friedlingstein, P., O'Sullivan, M., Jones, M. W., Andrew, R. M., Bakker, D. C. E., Hauck, J., Landschützer, P., Le Quéré, C., Li, H., Luijkx, I. T., Peters, G. P., Peters, W., Pongratz, J., Schwingshackl, C., Sitch, S., Canadell, J. G., Ciais, P., Aas, K., Alin, S. R., Anthoni, P., Barbero, L., Bates, N. R., Bellouin, N., Benoit-Cattin, A., Berghoff, C. F., Bernardello, R., Bopp, L., Brasika, I. B. M., Chamberlain, M. A., Chandra, N., Chevallier, F., Chini, L. P., Collier, N. O., Colligan, T. H., Cronin, M., Djeutchouang, L. M., Dou, X., Enright, M. P., Enyo, K., Erb, M., Evans, W., Feely, R. A., Feng, L., Ford, D. J., Foster, A., Fransner, F., Gasser, T., Gehlen, M., Gkritzalis, T., Goncalves De Souza, J., Grassi, G., Gregor, L., Gruber, N., Guenet, B., Gürses, Ö., Harrington, K., Harris, I., Heinke, J., Hurtt, G. C., Iida, Y., Ilyina, T., Ito, A., Jacobson, A. R., Jain, A. K., Jarníková, T., Jersild, A., Jiang, F., Jones, S. D., Kato, E., Keeling, R. F., Klein Goldewijk, K., Knauer, J., Kong, Y., Korsbakken, J. I., Koven, C.,

https://doi.org/10.5194/essd-2026-496
Preprint. Discussion started: 31 July 2026

Kunimitsu, T., Lan, X., Liu, J., Liu, Z., Liu, Z., Lo Monaco, C., Ma, L., Marland, G., McGuire, P. C., McKinley, G. A., Melton, J. R., Monacci, N., Monier, E., Morgan, E. J., Munro, D. R., Müller, J. D., Nakaoka, S.-I., Nayagam, L. R., Niwa, Y., Nutzel, T., Olsen, A., Omar, A. M., Pan, N., Pandey, S., Pierrot, D., Qin, Z., Regnier, P., Rehder, G., Resplandy, L., Roobaert, A., Rosan, T. M., Rödenbeck, C., Schwinger, J., Skjelvan, I., Smallman, T. L., Spada, V., Sreeush, M. G., Sun, Q., Sutton, A. J., Sweeney, C., Swingedouw, D., Séférian, R., Takao, S., Tatebe, H., Tian, H., Tian, X., Tilbrook, B., Tsujino, H., Tubiello, F., van Ooijen, E., van der Werf, G. R., van de Velde, S. J., Walker, A. P., Wanninkhof, R., Yang, X., Yuan, W., Yue, X., and Zeng, J.: Global Carbon Budget 2025, Earth Syst. Sci. Data, 18, 3211–3288, https://doi.org/10.5194/essd-18-3211-2026, 2026.

Friis, K., Körtzinger, A., & Wallace, D. W. (2003). The salinity normalization of marine inorganic carbon chemistry data. *Geophysical Research Letters*, *30*(2). https://doi.org/10.1029/2002GL015898

GLODAP Github. (2026). GLODAP Repository. Retrieved from https://github.com/GLODAP/glodap.github.io (last accessed 26.06.2026).

Good, S.A., Mills, B., Boyer, T., Bringas, F., Castelão, G.P., Cowley, R., Domingues, C.M., Gouretski, V., Reseghetti, F., Schumacher, C. and Simoncelli, S., 2023. Quality control of ocean temperature profiles in the EN4 dataset. Journal of Atmospheric and Oceanic Technology, 40(10), pp.1345–1363. Available at: https://doi.org/10.1175/JTECH-D-22-0119.1.

Gouretski, V. V. and Jancke, K.: Systematic errors as the cause for an apparent deep water property variability: global analysis of the WOCE and historical hydrographic data, Progress in Oceanography, 48, 337–402, 2001. https://doi.org/10.1016/S0079-6611(00)00049-5

Gregor, L. and Gruber, N.: OceanSODA-ETHZ: a global gridded data set of the surface ocean carbonate system for seasonal to decadal studies of ocean acidification, Earth Syst. Sci. Data, 13, 777–808, 10.5194/essd-13-777-2021, 2021.

Heuzé, C., Huhn, O., Walter, M., Sukhikh, N., Karam, S., Körtke, W., Vredenborg, M., Bulsiewicz, K., Sültenfuß, J., Fang, Y.-C., Mertens, C., Rabe, B., Tippenhauer, S., Allerholt, J., He, H., Kuhlmey, D., Kuznetsov, I., and Mallet, M.: A year of transient tracers (chlorofluorocarbon 12 and sulfur hexafluoride), noble gases (helium and neon), and tritium in the Arctic Ocean from the MOSAiC expedition (2019–2020), Earth Syst. Sci. Data, 15, 5517–5534. https://doi.org/10.5194/essd-15-5517-2023, 2023.

Humphreys, M. P., Lewis, E. R., Sharp, J. D., and Pierrot, D. (2022). PyCO2SYS v1.8: marine carbonate system calculations in Python. Geoscientific Model Development 15, 15-43. doi:10.5194/gmd-15-15-2022.

Humphreys, M. P., Lauvset, S. K., Lange, N., Bittig, H. C., Carter, B. R., Hoppema, M., Murata, A., Olsen, A., Tanhua, T., Ulfsbo, A., Velo, A., Woosley, R. J., Azetsu-Scott, K., Müller, J. D., and Pérez, F. F.: Furthest-first inversion for internal consistency adjustments in the biogeochemical data product GLODAPv3, EGUsphere [preprint], https://doi.org/10.5194/egusphere-2026-3063, 2026.

IOCCP-JAMSTEC 2018 Inter-laboratory Calibration Exercise of a Certified Reference Materials for Nutrients in Seawater. https://www.ioccp.org/images/06Nutrients/IOCCP_JAMSTEC_IC2018report180903protected.pdf

IPCC, 2021: Climate Change 2021: The Physical Science Basis. Contribution of Working Group I to the Sixth Assessment Report of the Intergovernmental Panel on Climate Change [Masson-Delmotte, V., P. Zhai, A. Pirani, S.L. Connors, C. Péan, S. Berger, N. Caud, Y. Chen, L. Goldfarb, M.I. Gomis, M. Huang, K. Leitzell, E. Lonnoy, J.B.R. Matthews, T.K. Maycock, T. Waterfield, O. Yelekçi, R. Yu, and B. Zhou (eds.)]. Cambridge University Press, Cambridge, United Kingdom and New York, NY, USA, 2391 pp. doi:10.1017/9781009157896

Jiang, L.-Q., Pierrot, D., Wanninkhof, R., Feely, R. A., Tilbrook, B., Alin, S., Barbero, L., Byrne, R. H., Carter, B. R., Dickson, A. G., Gattuso, J.-P., Greeley, D., Hoppema, M., Humphreys, M. P., Karstensen, J., Lange, N., Lauvset, S. K., Lewis, E. R., Olsen, A., Pérez, F. F., Sabine, C., Sharp, J. D., Tanhua, T., Trull, T. W., Velo, A., Allegra, A. J., Barker, P., Burger, E., Cai, W.-J., Chen, C.-T. A., Cross, J., Garcia, H., Hernandez-Ayon, J. M., Hu, X., Kozyr, A., Langdon, C., Lee, K., Salisbury, J., Wang, Z. A., and Xue, L.: Best Practice Data Standards for Discrete Chemical Oceanographic Observations, Frontiers in Marine Science, 8, 10.3389/fmars.2021.705638, 2022.

https://doi.org/10.5194/essd-2026-496
Preprint. Discussion started: 31 July 2026

Johnson, G. C., Robbins, P. E., and Hufford, G. E.: Systematic adjustments of hydrographic sections for internal consistency, Journal of Atmospheric and Oceanic Technology, 18, 1234–1244, 10.1175/1520-0426(2001)018<1234:saohsf>2.0.co;2, 2001.

Joyce, T. and Corry, C.: Chapter 4. Hydrographic Data Formats, in Requirements for WOCE Hydrographic Programme Data Reporting, WOCE Hydrographic Programme Office, Woods Hole Oceanographic Institution, Woods Hole, MA, 1994.

Keppler, L., Landschützer, P., Lauvset, S. K., & Gruber, N. (2023). Recent trends and variability in the oceanic storage of dissolved inorganic carbon. Global Biogeochemical Cycles, 37, e2022GB007677. https://doi.org/10.1029/2022GB007677

Key, R. M., Kozyr, A., Sabine, C. L., Lee, K., Wanninkhof, R., Bullister, J. L., Feely, R. A., Millero, F. J., Mordy, C., and Peng, T. H.: A global ocean carbon climatology: Results from Global Data Analysis Project (GLODAP), Global Biogeochemical Cycles, 18, https://doi.org/10.1029/2004gb002247, 2004.

Key, R. M., Tanhua, T., Olsen, A., Hoppema, M., Jutterström, S., Schirnick, C., Van Heuven, S., Kozyr, A., Lin, X., Velo, A., Wallace, D. W. R., and Mintrop, L.: The CARINA data synthesis project: introduction and overview, Earth Syst. Sci. Data, 2, 105–121, 2010. https://doi.org/10.5194/essd-2-105-2010

Lange, N., Lauvset, S. K., Carter, B. R., Humphreys, M. P., Woosley, R. J., Olsen, A., Bittig, H. C., Kozyr, A., Álvarez, M., Azetsu-Scott, K., Becker, S., Brown, P. J., Cotrim da Cunha, L., Hoppema, M., Ishii, M., Jeansson, E., Murata, A., Müller, J. D., Pérez, F. F., Schirnick, C., Steinfeldt, R., Ulfsbo, A., Velo, A., Tanhua, T. (2026). The Global Ocean Data Analysis Project version 3 (GLODAPv3) – an internally consistent biogeochemical data product for the World Ocean (NCEI Accession 0315582). NOAA National Centers for Environmental Information. Unpublished Dataset. https://www.ncei.noaa.gov/archive/accession/0315582.

Lauvset, S. K. and Tanhua, T.: A toolbox for secondary quality control on ocean chemistry and hydrographic data, Limnol. Oceanogr. Meth., 13, 601–608, 10.1002/lom3.10050, 2015.

Lauvset, S. K., Lange, N., Tanhua, T., Bittig, H. C., Olsen, A., Kozyr, A., Álvarez, M., Azetsu-Scott, K., Brown, P. J., Carter, B. R., Cotrim da Cunha, L., Hoppema, M., Humphreys, M. P., Ishii, M., Jeansson, E., Murata, A., Müller, J. D., Pérez, F. F., Schirnick, C., Steinfeldt, R., Suzuki, T., Ulfsbo, A., Velo, A., Woosley, R. J., and Key, R. M.: The annual update GLODAPv2.2023: the global interior ocean biogeochemical data product, Earth Syst. Sci. Data, 16, 2047–2072, 10.5194/essd-16-2047-2024, 2024.

Lauvset, S. K., Lange, N., Tanhua, T., Bittig, H. C., Olsen, A., Kozyr, A., Alin, S., Álvarez, M., Azetsu-Scott, K., Barbero, L., Becker, S., Brown, P. J., Carter, B. R., da Cunha, L. C., Feely, R. A., Hoppema, M., Humphreys, M. P., Ishii, M., Jeansson, E., Jiang, L. Q., Jones, S. D., Lo Monaco, C., Murata, A., Müller, J. D., Pérez, F. F., Pfeil, B., Schirnick, C., Steinfeldt, R., Suzuki, T., Tilbrook, B., Ulfsbo, A., Velo, A., Woosley, R. J., and Key, R. M.: GLODAPv2.2022: the latest version of the global interior ocean biogeochemical data product, Earth Syst. Sci. Data, 14, 5543–5572, 10.5194/essd-14-5543-2022, 2022.

Lee, K., Kim, T.-W., Byrne, R. H., Millero, F. J., Feely, R. A., & Liu, Y.-M. (2010). The universal ratio of Boron to Chlorinity for the North Pacific and North Atlantic oceans. *Geochimica et Cosmochimica Acta*, *74*(6), 1801–1811. https://doi.org/10.1016/j.gca.2009.12.027

Liu, X., Patsavas, M. C., & Byrne, R. H. (2011). Purification and Characterization of meta-Cresol Purple for Spectrophotometric Seawater pH Measurements. *Environmental Science & Technology*, *45*(11), 4862–4868. https://doi.org/10.1021/es200665d

Lueker, T. J., Dickson, A. G., & Keeling, C. D. (2000). Ocean pCO_2 calculated from dissolved inorganic carbon, alkalinity, and equations for K_1 and K_2: validation based on laboratory measurements of CO_2 in gas and seawater at equilibrium. *Marine Chemistry*, *70*(1), 105–119. https://doi.org/10.1016/S0304-4203(00)00022-0

Garcia, H.E., Boyer, T.P., Locarnini, R.A., Mishonov, A.V., Reagan, J.R., Seidov, D., Baranova, O.K., Paver, C.R. and Smolyar, I.V. (2026). World Ocean Database 2023: A Foundational Data Resource for and by the Global Ocean and Coastal Communities. Scientific Data, 13, p. 35. doi: 10.1038/s41597-026-06957-2.

McDonagh, E., Barbero, L., Kramp, M., Purkey, S. G., Hernández-Guerra, A., Carter, B., Cimoli, L., Davila, X., Ishii, M., Sloyan, B. M., Schroeder, K., Firing, Y., Stocks, K., Álvarez, M., Arumi, C., Bodrossy, L., Caínzos,

https://doi.org/10.5194/essd-2026-496
Preprint. Discussion started: 31 July 2026

V., Cardin, V., Carracedo, L. I., Chomiak, L. N., Civitarese, G., Erickson, Z. K., Fernandez, D., Fontela, M., Foppert, A., Gebbie, G., Hoppema, M., Jeansson, E., Johnson, G. C., Lauvset, S. K., Martiny, A. C., Mercier, H., Nunoura, T., Pérez, F. F., Raes, E., Rocha, C., Steinfeldt, R., Shigemitsu, M., Talley, L. D., Tanhua, T., Thompson, L., Williams, B., Wu, Q. and Yokokawa, T. (in press). Changes in ocean heat, carbon content, ventilation and biology: A review of the second decade of GO-SHIP global repeat hydrography. Annual Review of Marine Science.

McLaughlin, K., Weisberg, S. B., Dickson, A. G., Hofmann, G. E., Newton, J. A., Aseltine-Neilson, D., et al. (2015). Core principles of the California Current Acidification Network: Linking chemistry, physics, and ecological effects. *Oceanography*, *28*(2), 160–169. https://doi.org/10.5670/oceanog.2015.39

Millero, F. J. (2007). The marine inorganic carbon cycle. *Chemical Reviews*, *107*(2), 308–341. https://doi.org/10.1021/cr0503557

Müller, J. D., Gruber, N., Carter, B., Feely, R., Ishii, M., Lange, N., Lauvset, S. K., Murata, A., Olsen, A., Pérez, F. F., Sabine, C., Tanhua, T., Wanninkhof, R., and Zhu, D.: Decadal Trends in the Oceanic Storage of Anthropogenic Carbon From 1994 to 2014, AGU Advances, 4, e2023AV000875, https://doi.org/10.1029/2023AV000875, 2023.

Müller, J. D., Gruber, N. (2034). Progression of ocean interior acidification over the industrial era.Sci. Adv.10,eado3103.https://doi.org/10.1126/sciadv.ado3103.

Newton, J.A., Feely, R.A., Jewett, E.B., Williamson, P. and Mathis, J., 2015. Global Ocean Acidification Observing Network: Requirements and Governance Plan. 2nd edn. GOA-ON. https://archimer.ifremer.fr/doc/00651/76343/.

Olsen, A., Key, R. M., van Heuven, S., Lauvset, S. K., Velo, A., Lin, X., et al. (2016). The Global Ocean Data Analysis Project version 2 (GLODAPv2) – an internally consistent data product for the world ocean. *Earth System Science Data*, *8*(2), 297–323. https://doi.org/10.5194/essd-8-297-2016

Olsen, A., Lange, N., Key, R. M., Tanhua, T., Álvarez, M., Becker, S., et al. (2019). GLODAPv2.2019 -- an update of GLODAPv2. *Earth System Science Data*, *11*(3), 1437–1461. https://doi.org/10.5194/essd-11-1437-2019

Olsen, A., Rajasakaren, B., Jeansson, E., Lauvset, S. K., Omar, A. M., and Becker, M.: In the Wake of Deeper Convection: Nonsteady State Anthropogenic Carbon in the Greenland Sea, Journal of Geophysical Research: Oceans, 129, e2023JC020462, https://doi.org/10.1029/2023JC020462, 2024.

Patsavas, M. C., Byrne, R. H., & Liu, X. (2013). Purification of meta-cresol purple and cresol red by flash chromatography: Procedures for ensuring accurate spectrophotometric seawater pH measurements. *Marine Chemistry*, *150*, 19–24. https://doi.org/10.1016/J.MARCHEM.2013.01.004

Pérez, F.F. and Fraga, F. (1987). Association constant of fluoride and hydrogen ions in seawater. Marine Chemistry, 21(2), pp.161–168. https://doi.org/10.1016/0304-4203(87)90036-3.

Pérez, F. F., López-Mozos, M., Fontela, M., García-Ibáñez, M. I., Fajar, N., Padín, X. A., Castaño-Carrera, M., de la Paz, M., Carracedo, L. I., Álvarez, M., Mercier, H., Lherminier, P., and Velo, A. (2026). Two decades of pHT measurements along the GO-SHIP A25 section in the North Atlantic, Earth Syst. Sci. Data, 18, 801–821. https://doi.org/10.5194/essd-18-801-2026.

Reagan, J. R., Garcia, H. E., Boyer, T. P., Baranova, O. K., Bouchard, C., Cross, S. L., Dukhovskoy, D., Grodsky, A., Locarnini, R. A., Mishonov, A. V., Paver, C. R., Seidov, D., and Wang, Z.: World Ocean Atlas 2023: Product Documentation. https://doi.org/10.25923/a78k-gq49, 2023.

Rousseeuw, P. J. (1987). Silhouettes: A graphical aid to the interpretation and validation of cluster analysis. Journal of Computational and Applied Mathematics, 20, 53–65. https://doi.org/10.1016/0377-0427(87)90125-7.

Sabine, C., Key, R. M., Kozyr, A., Feely, R. A., Wanninkhof, R., Millero, F. J., Peng, T.-H., Bullister, J. L., and Lee, K.: Global Ocean Data Analysis Project (GLODAP): Results and Data, ORNL/CDIAC-145, NDP-083, Carbon Dioxide Information Analysis Center, Oak Ridge National Laboratory, U.S. Department of Energy, Oak Ridge, TN, USA, https://www.pmel.noaa.gov/co2/files/ndp083.pdf (last access: 29 April 2024), 2005.

https://doi.org/10.5194/essd-2026-496
Preprint. Discussion started: 31 July 2026

Sharp, J. D., Pierrot, D., Humphreys, M. P., Epitalon, J. M., Orr, J. C., Lewis, E. R., & Wallace, D. W. R. (2020). CO2SYSv3 for MATLAB. Zenodo. doi:10.5281/zenodo.3950562.

Sharp, J. D., & Byrne, R. H. (2020). Interpreting measurements of total alkalinity in marine and estuarine waters in the presence of proton-binding organic matter. *Deep Sea Research Part I: Oceanographic Research Papers*, *165*, 103338. https://doi.org/10.1016/j.dsr.2020.103338

Sharp, J. D., & Byrne, R. H. (2021). Technical note: Excess alkalinity in carbonate system reference materials. *Marine Chemistry*, *233*, 103965. https://doi.org/10.1016/j.marchem.2021.103965

Smith, S.R., Alory, G., Andersson, A., Asher, W., Baker, A., Berry, D.I., Bourassa, M.A., Cronin, M.F., de Thonel d'Orgeix, L., Donlon, C., Gulev, S.K., Kent, E.C., Lean, H., Legler, D.M., Leitita, M., McPhaden, M.J., Merchant, C.J., Minnett, P.J., O'Carroll, A. and Yu, L., 2019. Ship-based observations for advancing comprehensive ocean-atmosphere research. Frontiers in Marine Science, 6, p.434. https://doi.org/10.3389/fmars.2019.00434.

Stendardo, I., and Gruber, N. (2012). Oxygen trends over five decades in the North Atlantic, J. Geophys. Res., 117, C11004, doi:10.1029/2012JC007909.

Swift, J. and Diggs, S. C.: Description of WHP exchange format for CTD/Hydrographic data, CLIVAR and Carbon Hydrographic Data Office, UCSD Scripps Institution of Oceanography, San Diego, CA, US, https://cchdo.github.io/hdo-assets/documentation/WHP_Exchange_Description.pdf (last access: 29 April 2024), 2008.

Swift, J.: Reference-quality water sample data: Notes on acquisition, record keeping, and evaluation, in: The GO-SHIP Repeat Hydrography Manual: A Collection of Expert Reports and Guidelines, edited by: Hood, E. M., Sabine, C., and Sloyan, B. M., IOCCP Report Number 14, ICPO Publication Series Number 134, 2010. https://doi.org/10.25607/OBP-1346

Talley, L. D., Feely, R. A., Sloyan, B. M., Wanninkhof, R., Baringer, M. O., Bullister, J. L., Carlson, C. A., Doney, S. C., Fine, R. A., Firing, E., Gruber, N., Hansell, D. A., Ishii, M., Johnson, G. C., Katsumata, K., Key, R. M., Kramp, M., Langdon, C., Macdonald, A. M., Mathis, J. T., McDonagh, E. L., Mecking, S., Millero, F. J., Mordy, C. W., Nakano, T., Sabine, C. L., Smethie, W. M., Swift, J. H., Tanhua, T., Thurnherr, A. M., Warner, M. J., and Zhang, J. Z.: Changes in Ocean Heat, Carbon Content, and Ventilation: A Review of the First Decade of GO-SHIP Global Repeat Hydrography, Ann Rev Mar Sci, 8, 185–215, 10.1146/annurev-marine-052915-100829, 2016.

Tanhua, T., Van Heuven, S., Key, R. M., Velo, A., Olsen, A., and Schirnick, C.: Quality control procedures and methods of the CARINA database, Earth Syst. Sci. Data, 2, 205–240, 2010. https://doi.org/10.5194/essd-2-35-2010

Tanhua, T., Lauvset, S. K., Lange, N., Olsen, A., Álvarez, M., Diggs, S., Bittig, H. C., Brown, P. J., Carter, B. R., da Cunha, L. C., Feely, R. A., Hoppema, M., Ishii, M., Jeansson, E., Kozyr, A., Murata, A., Pérez, F. F., Pfeil, B., Schirnick, C., Steinfeldt, R., Telszewski, M., Tilbrook, B., Velo, A., Wanninkhof, R., Burger, E., O'Brien, K., and Key, R. M.: A vision for FAIR ocean data products, Communications Earth & Environment, 2, 136, 10.1038/s43247-021-00209-4, 2021.

Takeshita, Y., Warren, J. K., Liu, X., Spaulding, R. S., Byrne, R. H., Carter, B. R., et al. (2021). Consistency and stability of purified meta-cresol purple for spectrophotometric pH measurements in seawater. *Marine Chemistry*, *236*(July), 104018. https://doi.org/10.1016/j.marchem.2021.104018

Uppström, L. R. (1974). The boron/chlorinity ratio of deep-sea water from the Pacific Ocean. *Deep Sea Research and Oceanographic Abstracts*, *21*(2), 161–162. https://doi.org/10.1016/0011-7471(74)90074-6

Velo, A., Cacabelos, J., Lange, N., Perez, F. F., and Tanhua, T.: Ocean Data QC: Software package for quality control of hydrographic sections (v1.4.0), Zenodo [code], https://doi.org/10.5281/zenodo.4532402, 2021. '

Wilkinson, M. D., Dumontier, M., Aalbersberg, I. J., Appleton, G., Axton, M., Baak, A., Blomberg, N., Boiten, J.-W., da Silva Santos, L. B., Bourne, P. E., Bouwman, J., Brookes, A. J., Clark, T., Crosas, M., Dillo, I., Dumon, O., Edmunds, S., Evelo, C. T., Finkers, R., Gonzalez-Beltran, A., Gray, A. J. G., Groth, P., Goble, C., Grethe, J. S., Heringa, J., 't Hoen, P. A. C., Hooft, R., Kuhn, T., Kok, R., Kok, J., Lusher, S. J., Martone, M. E., Mons, A., Packer, A. L., Persson, B., Rocca-Serra, P., Roos, M., van Schaik, R., Sansone, S.-A., Schultes, E., Sengstag, T., Slater, T., Strawn, G., Swertz, M. A., Thompson, M., van der Lei, J., van Mulligen, E., Velterop, J., Waagmeester,

https://doi.org/10.5194/essd-2026-496
Preprint. Discussion started: 31 July 2026

A., Wittenburg, P., Wolstencroft, K., Zhao, J., and Mons, B.: The FAIR Guiding Principles for scientific data management and stewardship, Scientific Data, 3, 160018, 10.1038/sdata.2016.18, 2016.

Williams, N. L., Juranek, L. W., Feely, R. A., Johnson, K. S., Sarmiento, J. L., Talley, L. D., Dickson, A. G., Gray, A. R., Wanninkhof, R. Russel, J. L., Riser, S. C., and Takeshita, Y. (2017). Calculating surface ocean pCO2 from biogeochemical Argo floats equipped with pH: An uncertainty analysis, Global Biogeochem. Cy., 31, 591–604. https://doi.org/10.1002/2016GB005541.

Wong, A. P. S., Wijffels, S. E., Riser, S. C., Pouliquen, S., Hosoda, S., Roemmich, D., Gilson, J., Johnson, G. C., Martini, K., Murphy, D. J., Scanderbeg, M., Bhaskar, T. V. S. U., Buck, J. J. H., Merceur, F., Carval, T., Maze, G., Cabanes, C., André, X., Poffa, N., Yashayaev, I., Barker, P. M., Guinehut, S., Belbéoch, M., Ignaszewski, M., Baringer, M. O. N., Schmid, C., Lyman, J. M., McTaggart, K. E., Purkey, S. G., Zilberman, N., Alkire, M. B., Swift, D., Owens, W. B., Jayne, S. R., Hersh, C., Robbins, P., West-Mack, D., Bahr, F., Yoshida, S., Sutton, P. J. H., Cancouët, R., Coatanoan, C., Dobbler, D., Juan, A. G., Gourrion, J., Kolodziejczyk, N., Bernard, V., Bourlès, B., Claustre, H., D'Ortenzio, F., Le Reste, S., Le Traon, P.-Y., Rannou, J.-P., Saout-Grit, C., Speich, S., Thierry, V., Verbrugge, N., Angel-Benavides, I. M., Klein, B., Notarstefano, G., Poulain, P.-M., Vélez-Belchí, P., Suga, T., Ando, K., Iwasaska, N., Kobayashi, T., Masuda, S., Oka, E., Sato, K., Nakamura, T., Sato, K., Takatsuki, Y., Yoshida, T., Cowley, R., Lovell, J. L., Oke, P. R., van Wijk, E. M., Carse, F., Donnelly, M., Gould, W. J., Gowers, K., King, B. A., Loch, S. G., Mowat, M., Turton, J., Rama Rao, E. P., Ravichandran, M., Freeland, H. J., Gaboury, I., Gilbert, D., Greenan, B. J. W., Ouellet, M., Ross, T., Tran, A., Dong, M., Liu, Z., Xu, J., Kang, K., Jo, H., Kim, S.-D., and Park, H.-M.: Argo Data 1999–2019: Two Million Temperature-Salinity Profiles and Subsurface Velocity Observations From a Global Array of Profiling Floats, Frontiers in Marine Science, Volume 7 - 2020, 10.3389/fmars.2020.00700, 2020.

Woosley, R. J. (2021). Evaluation of the temperature dependence of dissociation constants for the marine carbon system using pH and certified reference materials. *Marine Chemistry*, *229*, 103914. https://doi.org/10.1016/j.marchem.2020.103914

Woosley, R. J., & Moon, J. Y. (2023). Re-evaluation of carbonic acid dissociation constants across conditions and the implications for ocean acidification. *Marine Chemistry*, *250*(April), 104247. https://doi.org/10.1016/j.marchem.2023.104247

Woosley, R. J., Bruno, J. A., Neithardt, D., Wang, Zhaohui. A., Fujiki, N., Shigemitsu, M., & Murata, A. (2025). Comparison of open cell and single-step total alkalinity titration methods and implications for organic alkalinity. *Limnology and Oceanography: Methods*. https://doi.org/10.1002/lom3.70002

Yao, W., Liu, X., & Byrne, R. H. (2007). Impurities in indicators used for spectrophotometric seawater pH measurements: Assessment and remedies. *Marine Chemistry*, *107*(2), 167–172. https://doi.org/10.1016/J.MARCHEM.2007.06.012